Form Factor Prospects with a 22 GeV CEBAF (Nucleon/Pion/etc)

Andrew Puckett
University of Connecticut

Science at the Luminosity Frontier: Jefferson Lab at 22 GeV Workshop

January 24, 2023

UCONN

Acknowledgements

- DOE Office of Science, Office of Nuclear Physics, Award DE-SC0021200
- Additional support from Jefferson Lab and UConn
- Garth Huber for providing helpful material on pion/kaon FFs

Elastic Electron-Nucleon Scattering and Form Factors

- The Dirac (F_1) and Paul (F_2) form factors describe the most general form of the virtual photon-nucleon vertex function consistent with the symmetries of QED; namely, Lorentz invariance, parity conservation and gauge invariance/current conservation
- They are real-valued functions of the (space-like) squared four-momentum transfer $q^2 = (k - k')^2 < 0$.
- Experimental observables sensitive to form factors include differential cross sections and double-spin asymmetries involving polarized e^- beams and/or targets

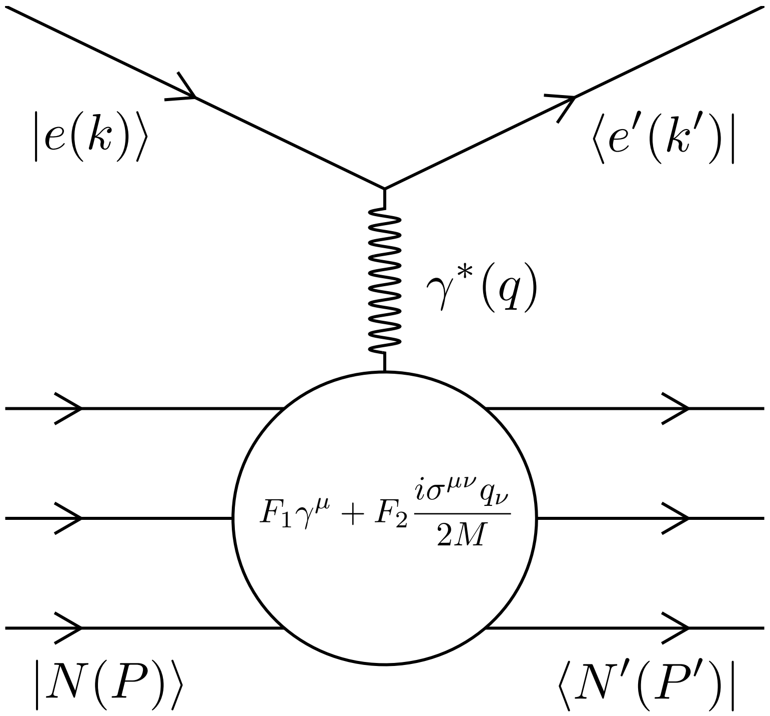

Feynman Diagram for elastic $eN \to eN$ scattering in OPE approximation

$$\begin{aligned}
\text{Invariant amplitude: } \mathcal{M} &= 4\pi\alpha\bar{u}(k')\gamma^\mu u(k)\left(\frac{g_{\mu\nu}}{q^2}\right)\bar{u}(P')\Gamma^\nu u(P) \\
\gamma^* N \text{ vertex function: } \Gamma^\mu &= F_1(q^2)\gamma^\mu + \frac{i\sigma^{\mu\nu}q_\nu}{2M}F_2(q^2) \\
\text{Sachs FF: } G_E &= F_1 - \tau F_2 \\
G_M &= F_1 + F_2 \\
\text{Rosenbluth Formula: } \frac{d\sigma}{d\Omega_e} &= \left(\frac{d\sigma}{d\Omega_e}\right)_{\text{Mott}} \frac{\epsilon G_E^2 + \tau G_M^2}{\epsilon(1+\tau)}
\end{aligned}$$

$$\begin{aligned}
\tau &\equiv \frac{Q^2}{4M^2} \\
\epsilon &\equiv \left[1 + 2(1+\tau)\tan^2\left(\frac{\theta_e}{2}\right)\right]^{-1}
\end{aligned}$$

Elastic FFs for the pion (thanks to Garth Huber!)

Charged Pion Form Factor

University of Regina

- **The pion is attractive as a QCD laboratory:**
  - Simple, 2 quark system

- **The pion is the "positronium atom" of QCD, its form factor is a test case for most model calculations**
- **The important question to answer is: What is the structure of the π^+ at all Q^2?**

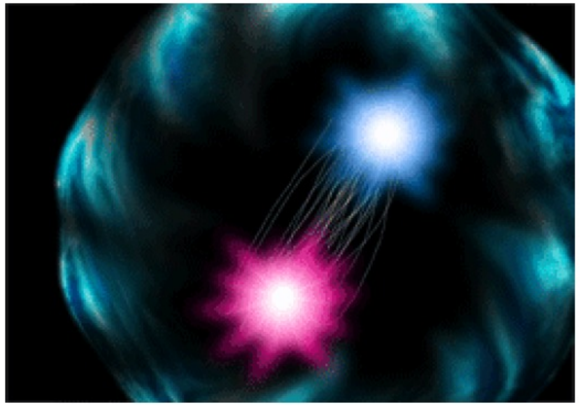

Pion's structure is determined by two valence quarks, and the quark-gluon sea.

- **A program of study unique to Jefferson Lab Hall C**
  (until the completion of the EIC)

Garth Huber, huberg@uregina.ca

Measurement of π^+ Form Factor – Larger Q^2

University of Regina

At larger Q^2, F_π must be measured indirectly using the "pion cloud" of the proton via pion electroproduction $p(e,e'\pi^+)n$

$$|p\rangle = |p\rangle_0 + |n\pi^+\rangle + \ldots$$

- At small $-t$, the pion pole process dominates the longitudinal cross section, σ_L
- In Born term model, $F_\pi^{\,2}$ appears as,

$$\boxed{\frac{d\sigma_L}{dt} \propto \frac{-tQ^2}{(t-m_\pi^2)}\, g_{\pi NN}^2(t)\, F_\pi^2(Q^2,t)}$$

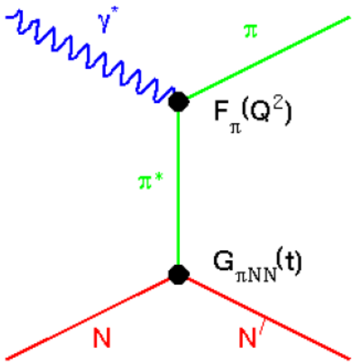

Drawbacks of this technique

1. Isolating σ_L experimentally challenging
2. Theoretical uncertainty in form factor extraction.

Garth Huber, huberg@uregina.ca

The Nobel Prize in Physics, 1961 (R. Hofstadter)

"for his pioneering studies of electron scattering in atomic nuclei and for his thereby achieved discoveries concerning the structure of the nucleons"

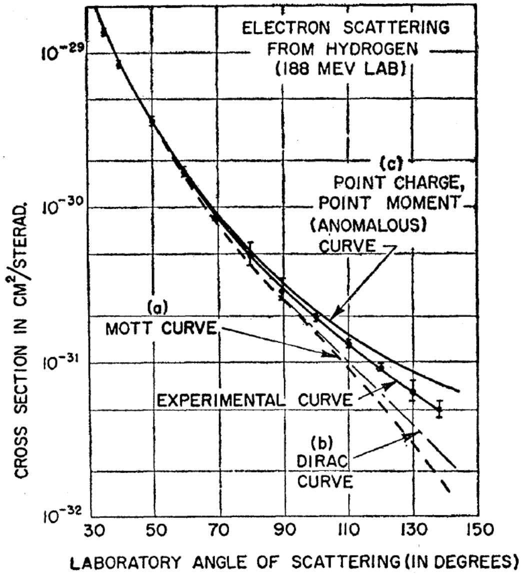

FIG. 24. Electron scattering from the proton at an incident energy of 188 Mev. The experimental points lie below the point-charge point-moment curve of Rosenbluth, indicating finite size effects.

Figures from [Rev. Mod. Phys, 28, 214 (1956)]

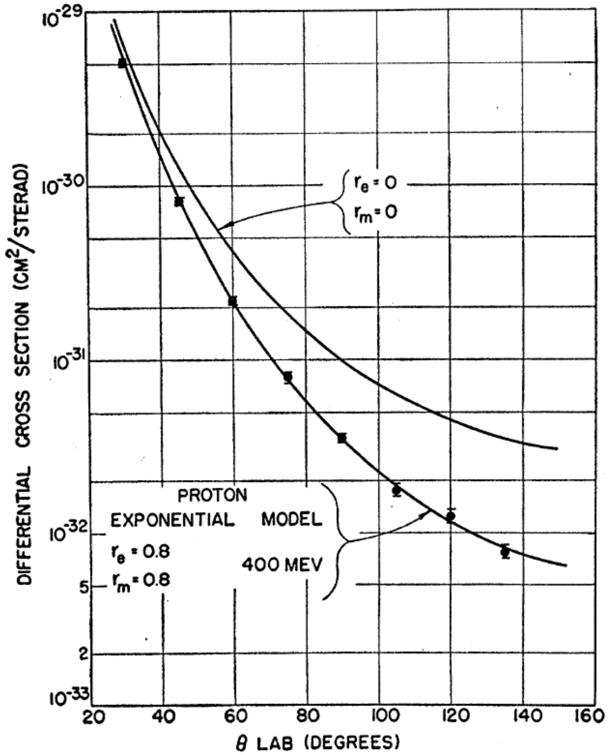

FIG. 26. Typical angular distribution for elastic scattering of 400-Mev electrons against protons. The solid line is a theoretical curve for a proton of finite extent. The model providing the theoretical curve is an exponential with rms radii$=0.80\times10^{-13}$ cm.

Proton Form Factors From Rosenbluth Separations

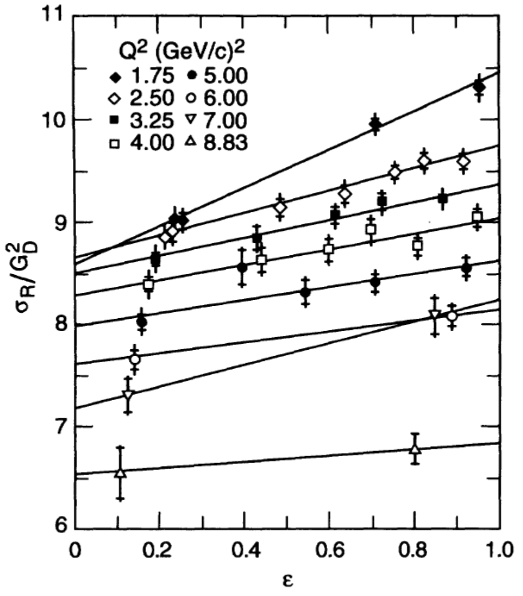

FIG. 22. Reduced cross sections divided by the square of the dipole fit plotted versus ϵ for each value of Q^2. The 1.6 GeV data points correspond to the leftmost point on each line, and the E136 data point is the rightmost point on the $Q^2 = 8.83\ (\mathrm{GeV}/c)^2$ line. The inner error bars show the statistical error, while the outer error bars show the total point-to-point uncertainty, given by the quadrature sum of the statistical and point-to-point systematic errors. An overall normalization uncertainty of ±1.77% has not been included.

NE11 L/T separations from Andivahis *et al.,* Phys. Rev. D 50, 5491 (1994)

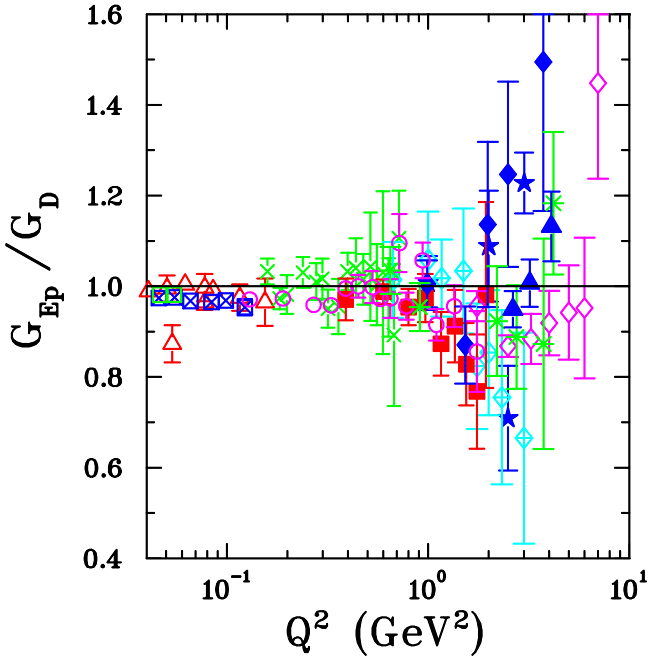

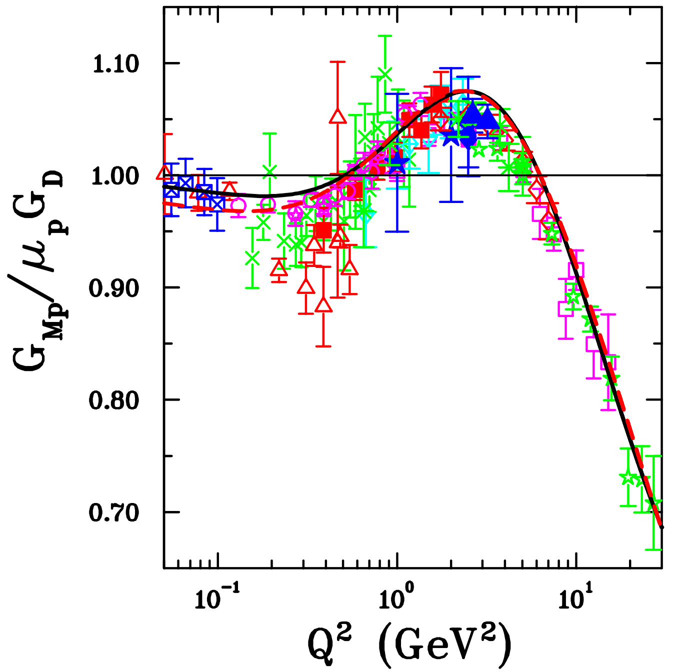

- **Above figures from Puckett *et al.* PRC 96, 055203 (2017)**
- Most proton electric and magnetic FF Rosenbluth extractions can be described to within ~10-20% over the entire measured Q^2 range by the so-called "dipole" form factor:

$$G_E^p \approx G_M^p/\mu_p \approx G_D \equiv \left(1 + \frac{Q^2}{\Lambda^2}\right)^{-2}$$

$$\Lambda^2 = 0.71\ (\mathrm{GeV/c})^2$$

The Problem with Rosenbluth Separations

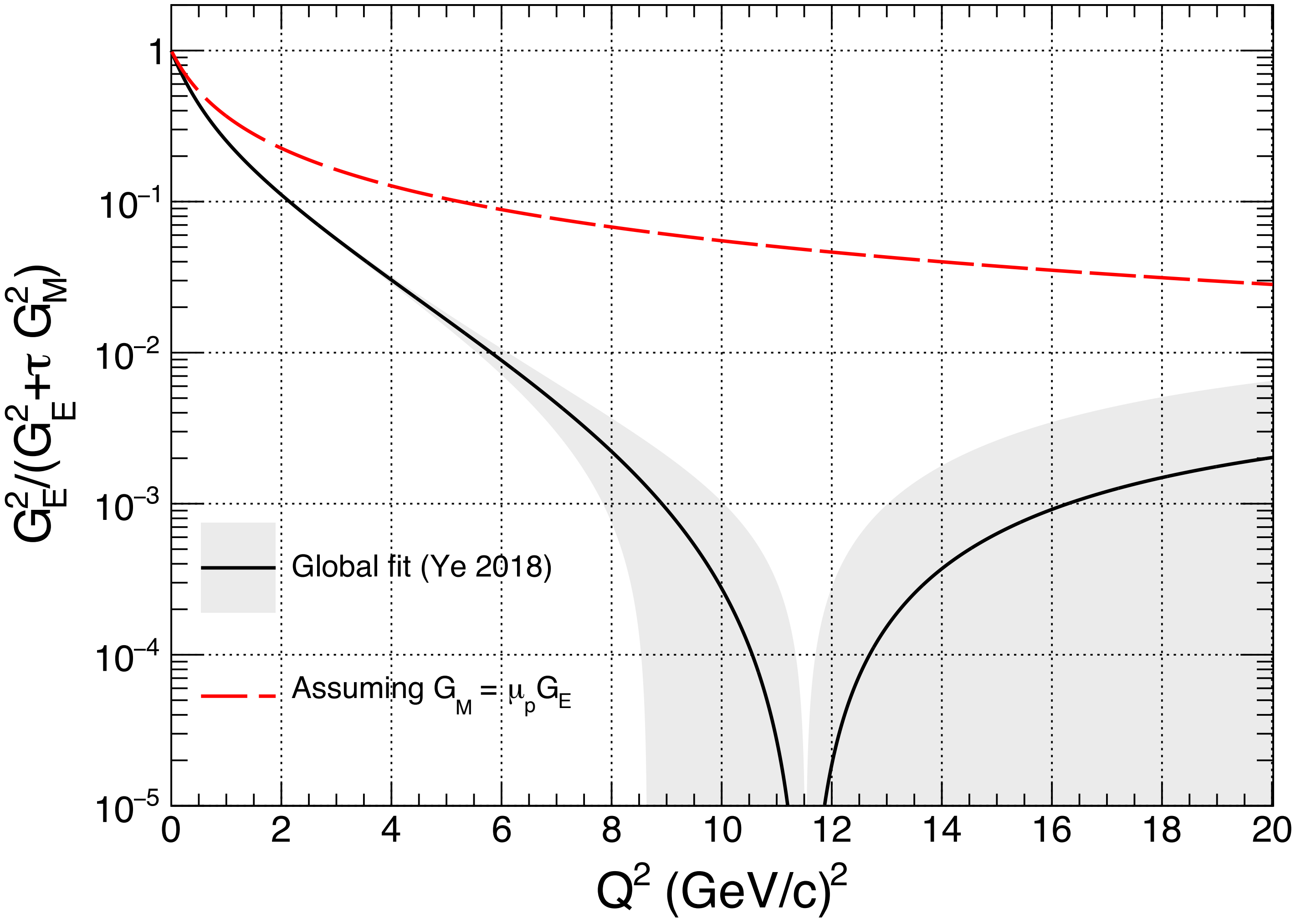

Maximum Fraction of the Reduced Cross Section Carried by the electric term versus Q^2

Polarization Observables in Elastic $eN \to eN$ Scattering

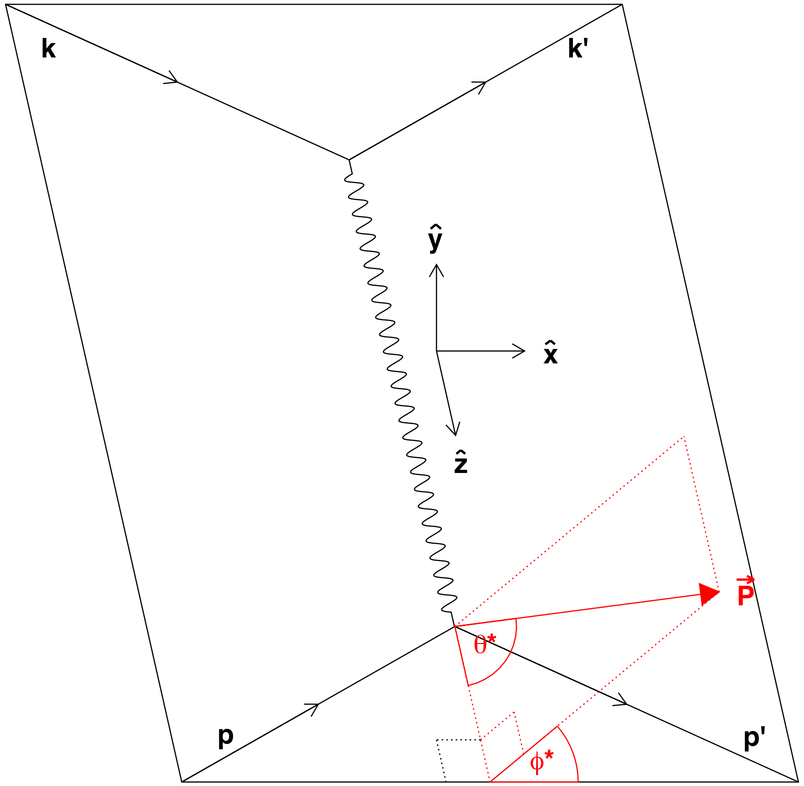

Standard coordinate system and angle definitions for nucleon polarization components in $eN \to eN$

$$A_{eN} \equiv \frac{\sigma_+ - \sigma_-}{\sigma_+ + \sigma_-} = P_{\text{beam}} P_{\text{targ}} \left[A_t \sin\theta^* \cos\phi^* + A_\ell \cos\theta^* \right]$$

$$A_t = -\sqrt{\frac{2\epsilon(1-\epsilon)}{\tau}} \frac{r}{1 + \frac{\epsilon}{\tau} r^2}$$

$$A_\ell = -\frac{\sqrt{1-\epsilon^2}}{1 + \frac{\epsilon}{\tau} r^2}$$

$$r \equiv \frac{G_E}{G_M}$$

$$P_t = P_{beam} A_t$$

$$P_\ell = -P_{beam} A_\ell$$

$$\frac{G_E}{G_M} = -\frac{P_t}{P_\ell} \sqrt{\frac{\tau(1+\epsilon)}{2\epsilon}} = -\frac{P_t}{P_\ell} \frac{E_e + E'_e}{2M} \tan\left(\frac{\theta_e}{2}\right)$$

- Polarized beam-polarized target double-spin asymmetry or polarization transfer observables in OPE are sensitive to the electric/magnetic form factor *ratio*, giving enhanced sensitivity to $G_E (G_M)$ for large (small) values of Q^2, as compared to the Rosenbluth method

Polarization Results for $\mu_p G_E^p / G_M^p$ and the 2017 Bonner Prize

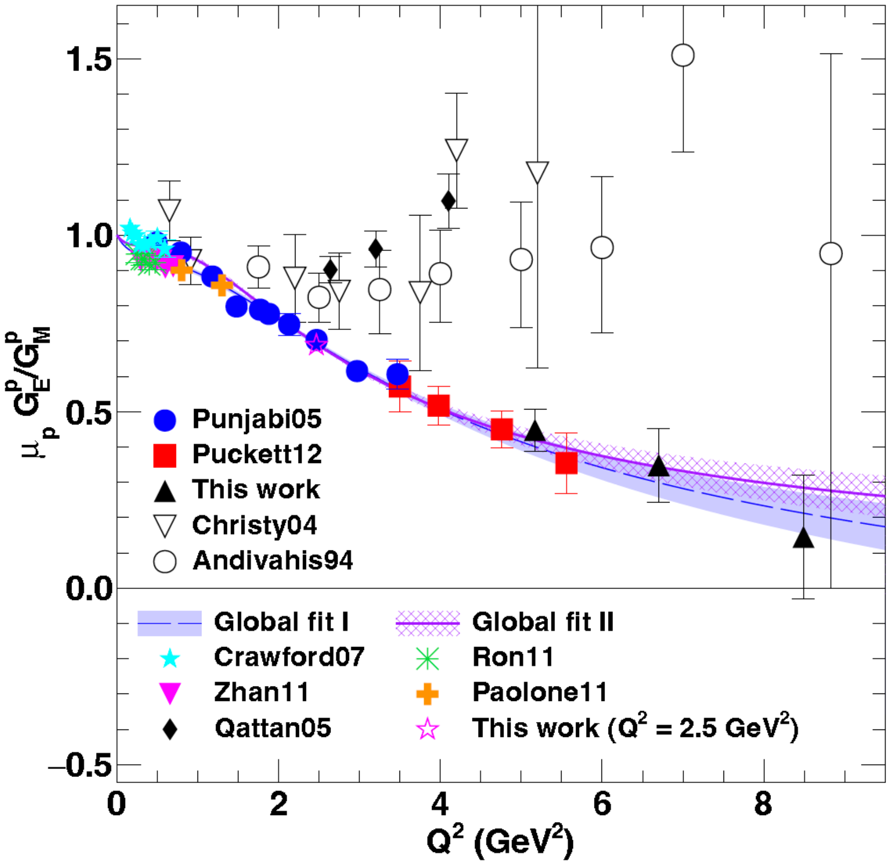

Figure from PRC 96, 055203 (2017)

References:

- GEp-I:
  - Jones, PRL 84, 1398 (2000)
  - Punjabi, PRC 71, 055202 (2005)
- GEp-II:
  - Gayou, PRL 88, 092301 (2002)
  - Puckett, PRC 85, 045203 (2012)
- GEp-III/GEp-2γ:
  - Puckett, PRL 104, 242301 (2010)
  - Meziane, PRL 106, 132501 (2011)
  - Puckett, PRC 96, 055203 (2017)

- (Arguably) most famous results in the history of JLab, among the most cited

2017 Tom W. Bonner Prize in Nuclear Physics Recipient

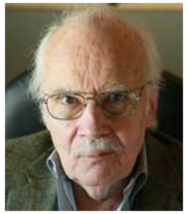

Charles F. Perdrisat
College of William and Mary

Citation:

"For groundbreaking measurements of nucleon structure, and discovering the unexpected behavior of the magnetic and electric nucleon form factors with changing momentum transfer."

Background:

Charles F. Perdrisat, Ph.D., was a professor at the College of William and Mary (Williamsburg, Va.) for the last 50 years having retired earlier this year. Throughout his career, Dr. Perdrisat's research focus included nuclear reactions with proton and deuteron beams, both polarized and unpolarized. He conducted research at SATURNE in Saclay, France, TRIUMF in Vancouver, B.C., LAMPF in Los Alamos, New Mexico, Brookhaven National Laboratory in Upton, N.Y., and JINR in Dubna, Russia. During the last half of his career, he was committed to the investigation of the structure of the proton at Jefferson Laboratory, concentrating in obtaining polarization transfer data in the scattering of polarized electrons on unpolarized protons. These data, from 3 distinct experiments organized in close collaboration with Vina Punjabi, Ph.D., Mark K. Jones, Ph.D., Edward J. Brash, Ph.D., and Lubomir Pentchev, Ph.D., have resulted in a significant change of paradigm in the understanding of the structure of the nucleon. After completing his undergraduate training in physics and mathematics at the University of Geneva in 1956, Dr. Perdrisat became an assistant in the physics department at the Swiss Federal Institute of Technology in Zurich) in Switzerland, under Prof. Paul Scherrer; he received his Ph.D. in 1962. He completed a three-year postdoctoral fellowship at the University of Illinois Urbana-Champaign, before heading to William and Mary in 1966.

Selection Committee:

2017 Selection Committee Members: Rocco Schiavilla (Chair), D. Hertzog, P. Jacobs, Kate Jones, I-Y. Lee

Theoretical Interpretation of Nucleon Elastic Form Factors

- Density interpretations:
  - G_E, G_M are 3D Fourier transforms of nucleon's charge and magnetic moment distributions (for low Q) in 3D space
  - At any Q, a model-independent density interpretation exists in which F_1 and F_2 are 2D Fourier-Bessel transforms of impact parameter-space densities in the infinite momentum frame (IMF)
- Perturbative QCD: for asymptotically large Q^2, form factor behavior is predicted by simple constituent counting rules; $F_1 \propto Q^{-4}, F_2 \propto \frac{F_1}{Q^2}$, assuming dominance of multiple hard-gluon exchange mechanism
- Constituent Quark Models—define quarks as effective degrees of freedom, solve bound-state Hamiltonian with confining quark-quark interaction, use wavefunction to predict FFs.
- Lattice QCD—Experiment far ahead of theory in precision, but data help to benchmark/improve the calculations
- Basis Light-Front Quantization
- Dyson-Schwinger Equations: approximate solutions of continuum non-perturbative QCD
- Model-independent constraints on Generalized Parton Distributions from FF data, evaluate sum rules for proton spin decomposition (quark and gluon spin and angular momentum)

Neutron Form Factors and Quark Flavor Decomposition

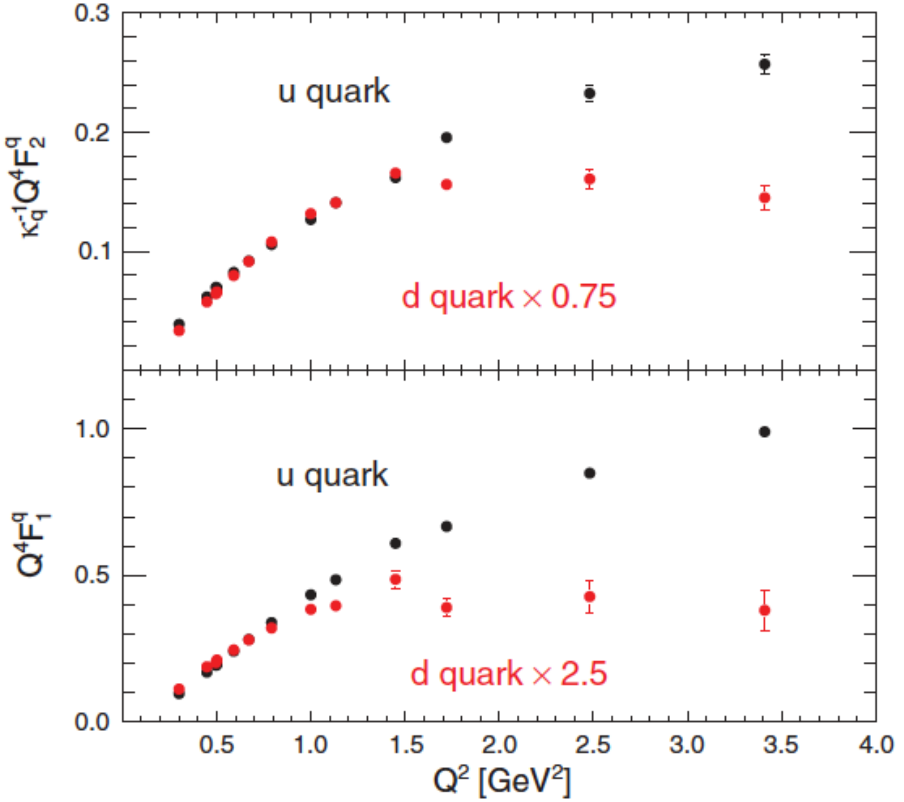

FIG. 3 (color). The Q^2 dependence for the u and d contributions to the proton form factors (multiplied by Q^4). The data points are explained in the text.

Cates *et al.*, PRL 106, 252003 (2011)

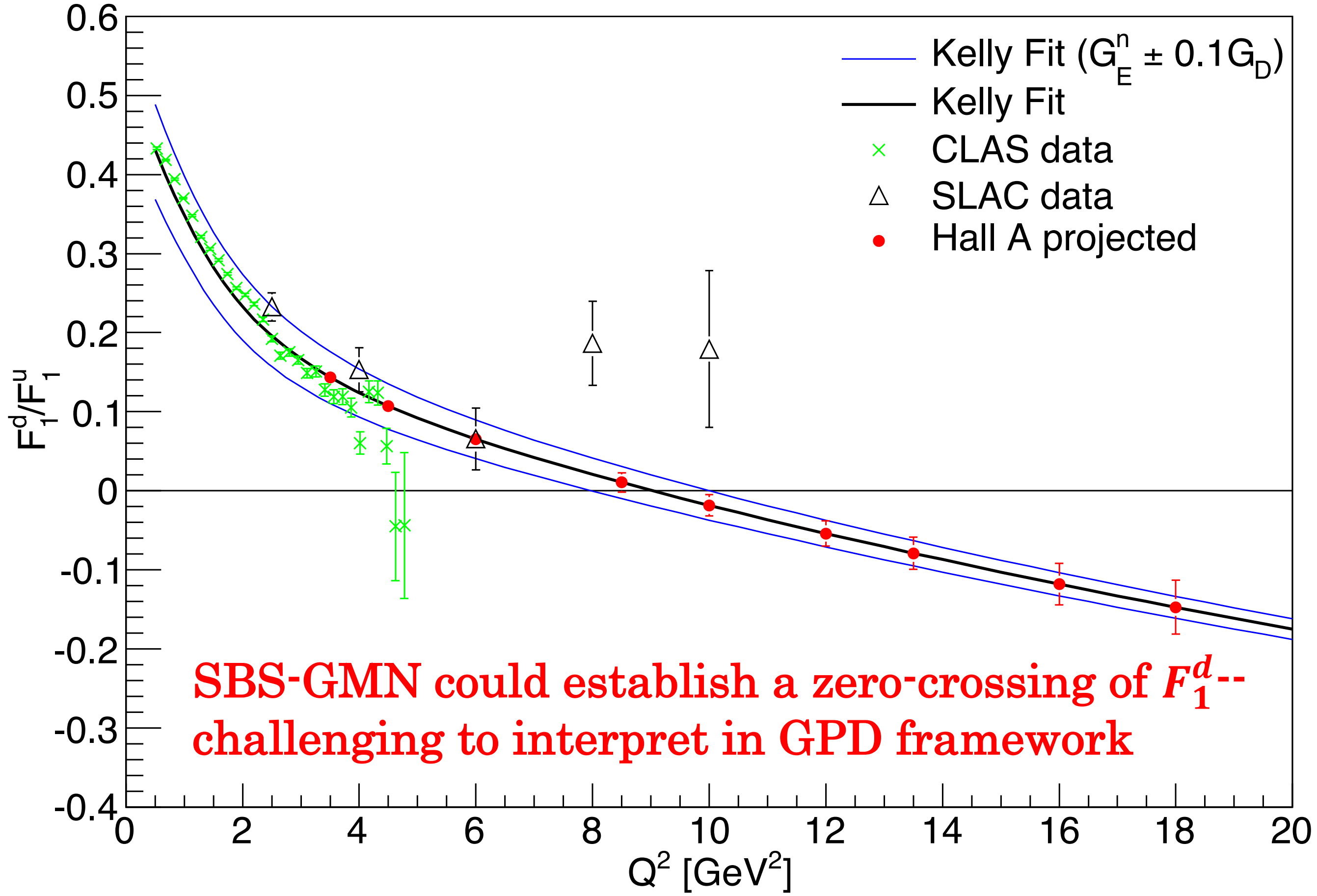

- Notable behaviors: d and u quark FFs show dramatically different Q^2 dependence.
- Flavor FF ratios F_2^q/F_1^q almost constant for both u and d above 1 GeV²

ECT* diquarks workshop, Trento, Sept. 23-27, 2019

Progress in Particle and Nuclear Physics 116 (2021) 103835

ELSEVIER

Contents lists available at ScienceDirect

Progress in Particle and Nuclear Physics

journal homepage: www.elsevier.com/locate/ppnp

Review

Diquark correlations in hadron physics: Origin, impact and evidence

Check for updates

M.Yu. Barabanov [1], M.A. Bedolla [2], W.K. Brooks [3], G.D. Cates [4], C. Chen [5], Y. Chen [6,7], E. Cisbani [8], M. Ding [9], G. Eichmann [10,11], R. Ent [12], J. Ferretti [13], R.W. Gothe [14], T. Horn [15,12], S. Liuti [4], C. Mezrag [16], A. Pilloni [9], A.J.R. Puckett [17], C.D. Roberts [18,19,*], P. Rossi [12,20], G. Salmé [21], E. Santopinto [22], J. Segovia [23,19], S.N. Syritsyn [24,25], M. Takizawa [26,27,28], E. Tomasi-Gustafsson [16], P. Wein [29], B.B. Wojtsekhowski [12]

[1] *Joint Institute for Nuclear Research, Dubna, 141980, Russia*

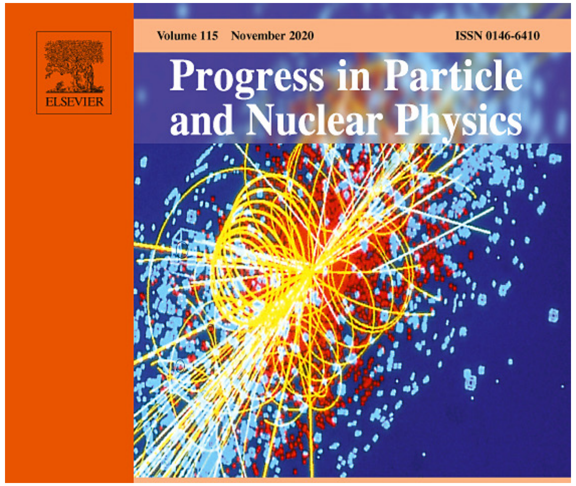

- High-Q^2 form factors are among the most sensitive experimental signatures of diquark correlations, now thought to play an important role in hadron structure; 2019 workshop brought together theorists and experimentalists at ECT* in Trento, Italy
- PPNP article now published as PPNP 116, 103835 (2021): https://doi.org/10.1016/j.ppnp.2020.103835

Continued relevance of high-Q^2 FF measurements

- For Q ~ few GeV we are probing the theoretically challenging and interesting region of transition between non-perturbative QCD, strong-coupling, and confinement to weak-coupling, asymptotic freedom, and pQCD.
- High sensitivity to running of momentum-dependent dressed quark mass function in the few-GeV regime
- In the high Q^2 regime the FF behavior is dominated by valence 3-quark Fock state, pion cloud suppressed, better discrimination among theoretical models→elucidate relevant degrees of freedom
- Precise FF knowledge at high Q^2 required both to directly constrain GPD moments and to interpret DVCS experiments

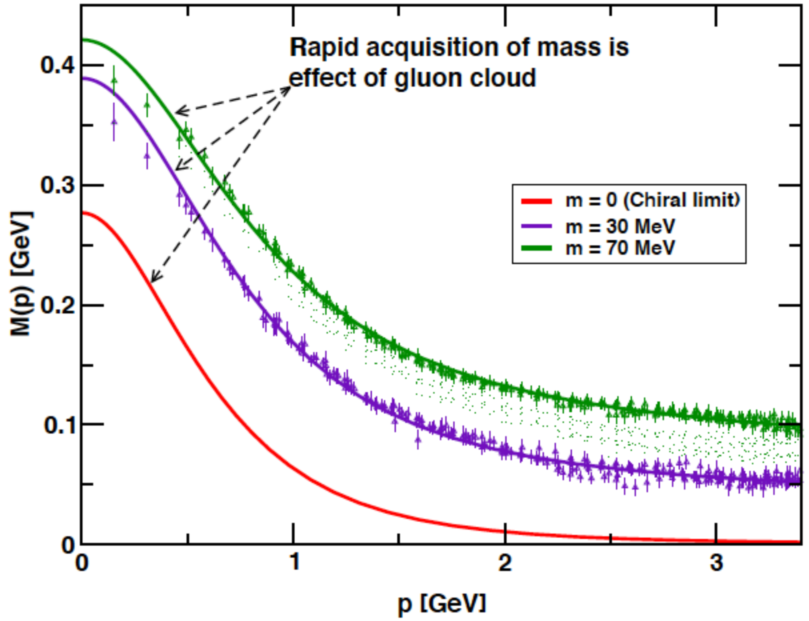

- Comparison of continuum and Lattice results for M(p)

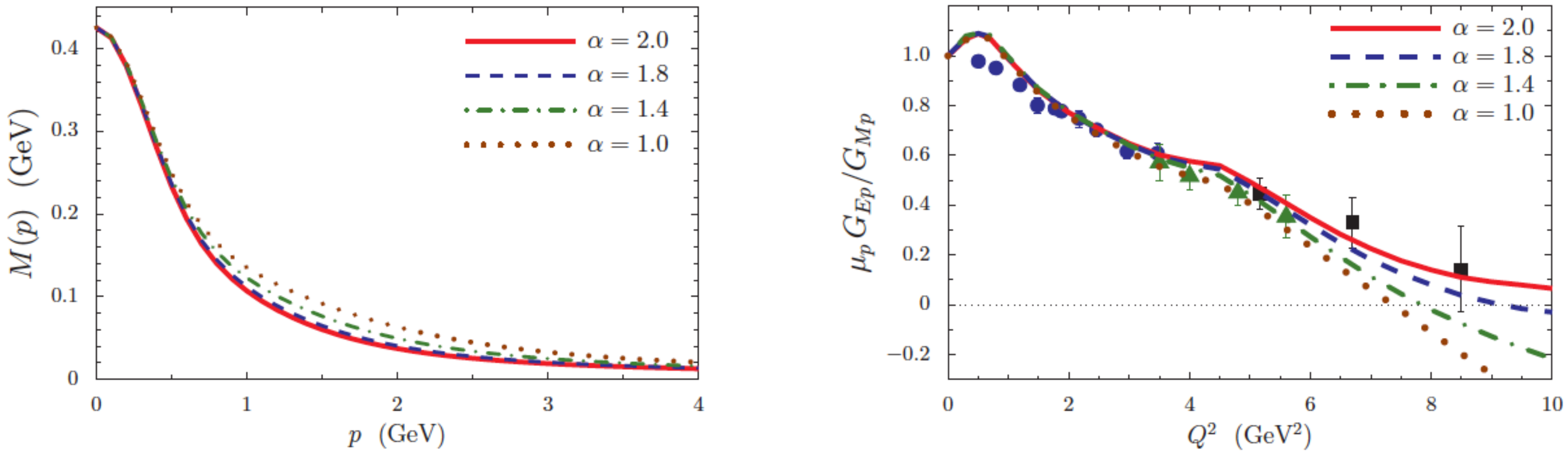

Figure 7.1: *Left panel.* Dressed-quark mass function employed in Ref. [89]. $\alpha = 1$ specifies the reference form and increasing α diminishes the domain upon which DCSB is active. *Right panel.* Response of $\mu_p G_E/G_M$ to increasing α; i.e., to an increasingly rapid transition between constituent- and parton-like behaviour of the dressed-quarks. Data are from Refs. [301, 312–316].

- High-Q^2 form factor behavior highly sensitive to M(p) in Dyson-Schwinger Equation (DSE) framework
- Cloet and Roberts, PPNP 77, 1 (2014)

Proton FF Existing Data Summary

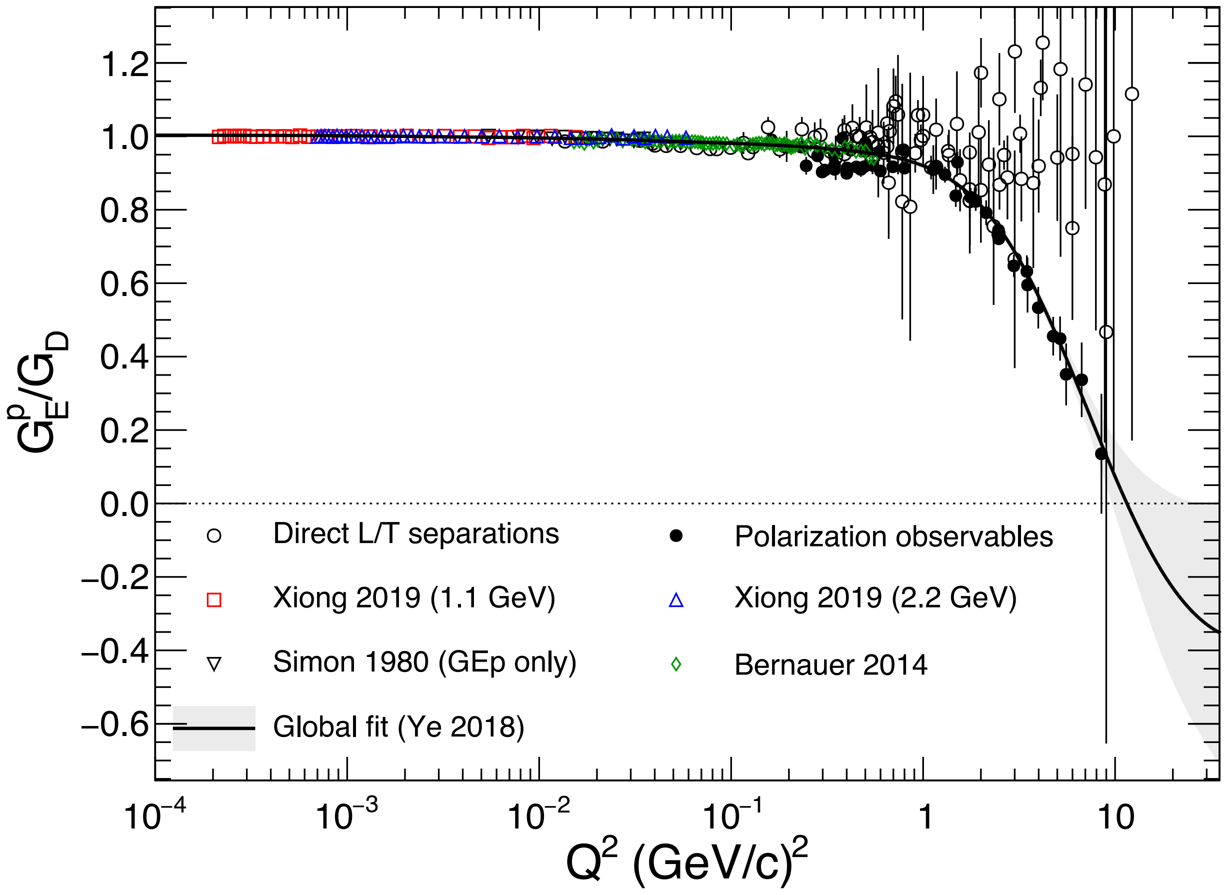

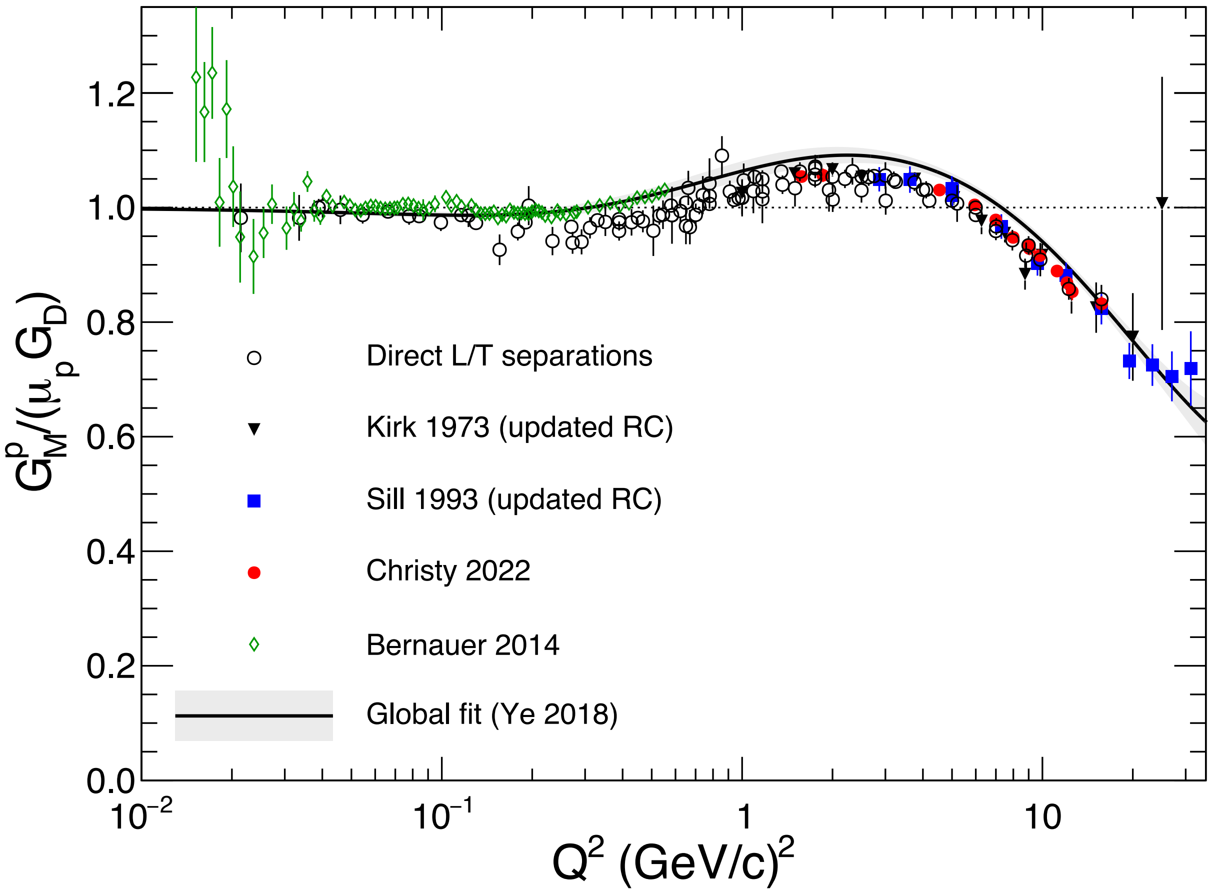

- Figures from FF mini-review in upcoming “50 Years of QCD” volume: https://arxiv.org/abs/2212.11107

Neutron FFs—GMN

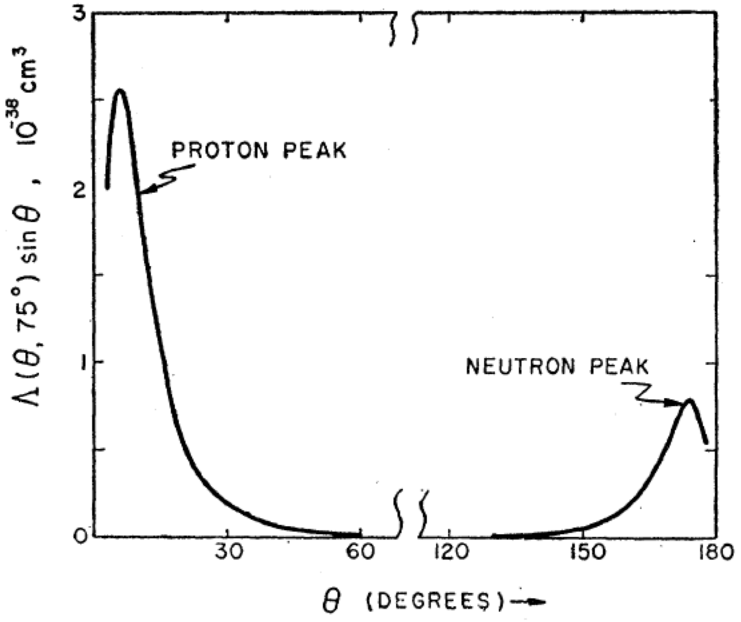

FIG. 1. The angular distribution function $\Lambda(\theta,\vartheta)\sin\theta$ in the absence of final-state interactions is plotted as a function of the proton scattering angle in the nucleon center-of-mass system $[\cos\theta = \hat{p}\cdot\hat{q}]$ for the scattering of 500-Mev electrons through an angle $\vartheta = 75°$ with a momentum transfer giving $p = \frac{1}{2}q = 1.3\times10^{13}$ cm^{-1}. $\Lambda(\theta,\vartheta)$ is defined in Eq. (11.2); the function $F(\theta)$ entering the definition was evaluated using a Hulthén wave function for the deuteron. The cross section $d^3\sigma/(d\theta d\Omega_e dE_e')$ is given by $(4.71\times10^5$ cm^{-1} rad^{-1} sterad^{-1} Mev$^{-1})$ $\Lambda(\theta,\vartheta)\sin\theta$. No nucleon form factors have been introduced into the results.

Ratio method: Durand, [Phys. Rev. 115, 1020 (1959)]

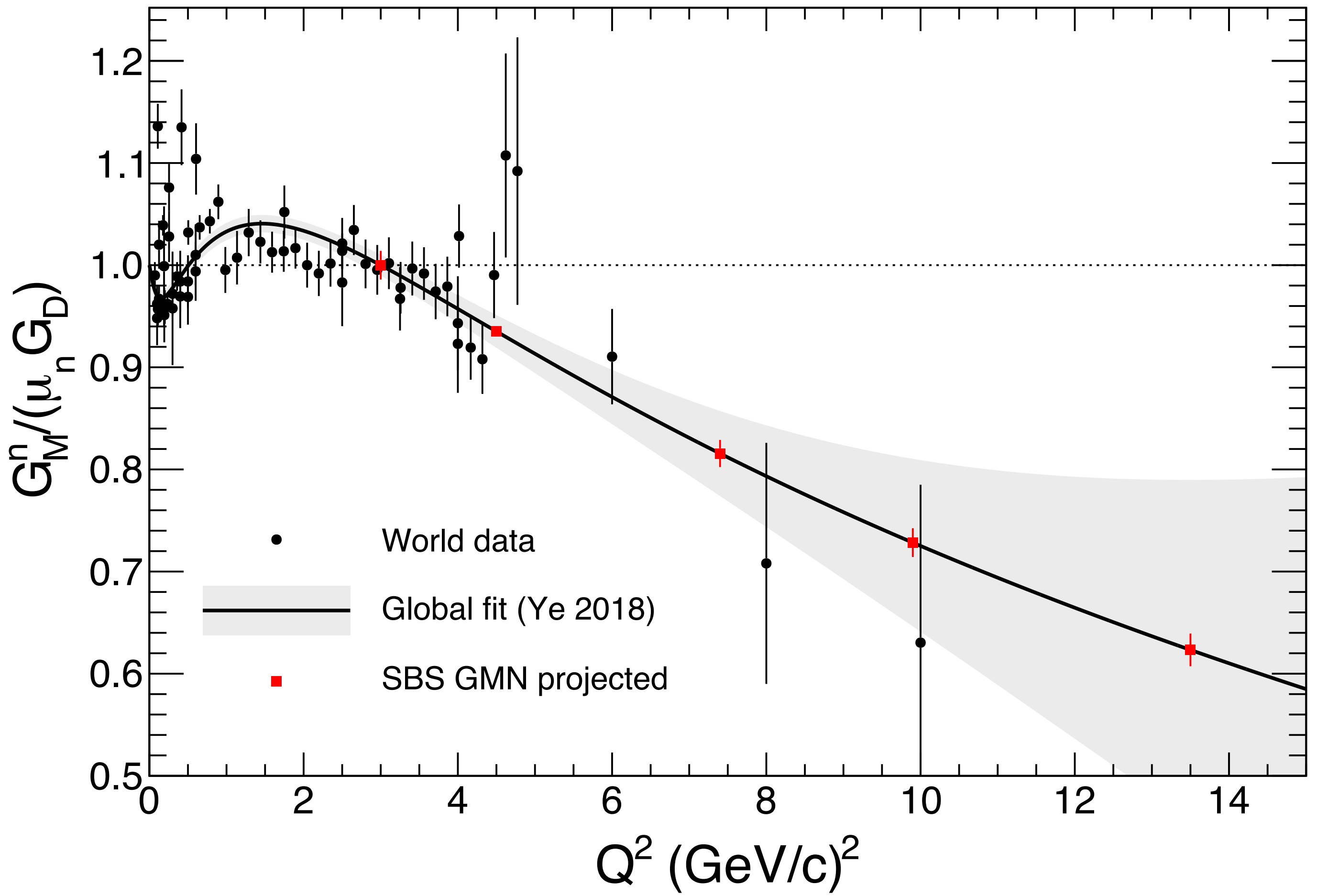

World data for $G_M^n/\mu_n G_D$ with **projected SBS accuracy** ***based on completed data taking 2021-2022***

Neutron FFs—GEN

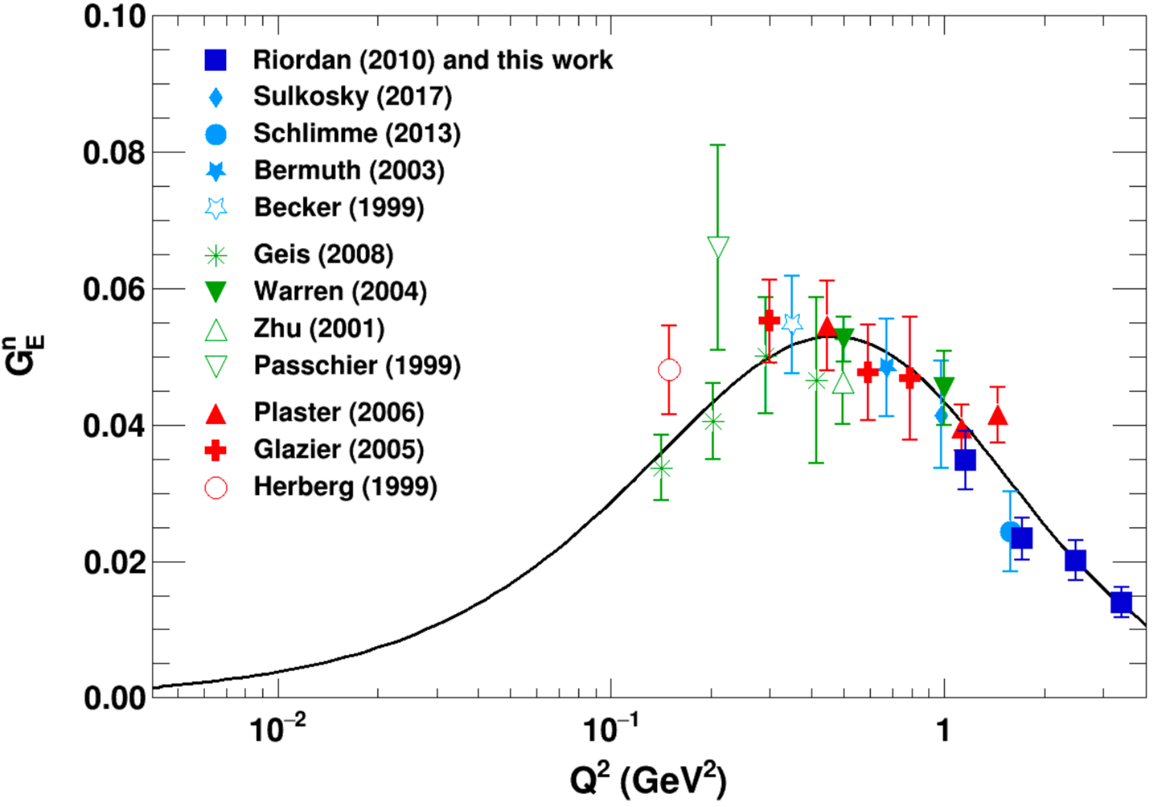

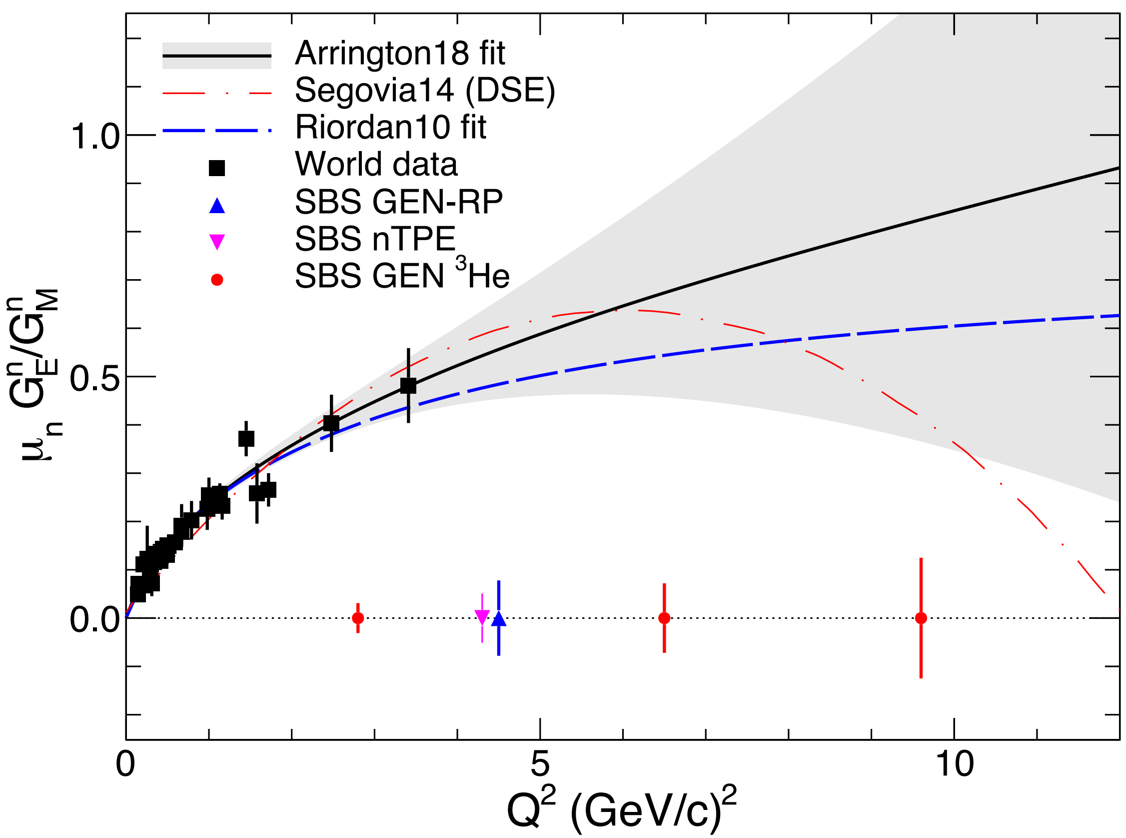

- Left (from Obrecht *et al.*, in preparation): G_E^n from polarization observables (color-coded by observable): Polarized Helium-3 target asymmetry, Deuteron recoil polarimetry, Polarized deuterium target asymmetry.
  - See Freddy Obrecht Ph.D. thesis: https://opencommons.uconn.edu/dissertations/2045/
- Right: GEN world data with projected SBS results, including already-collected Helium-3 data at 3 and 6.5 GeV²

The SBS high-Q^2 Form Factor Program in Hall A

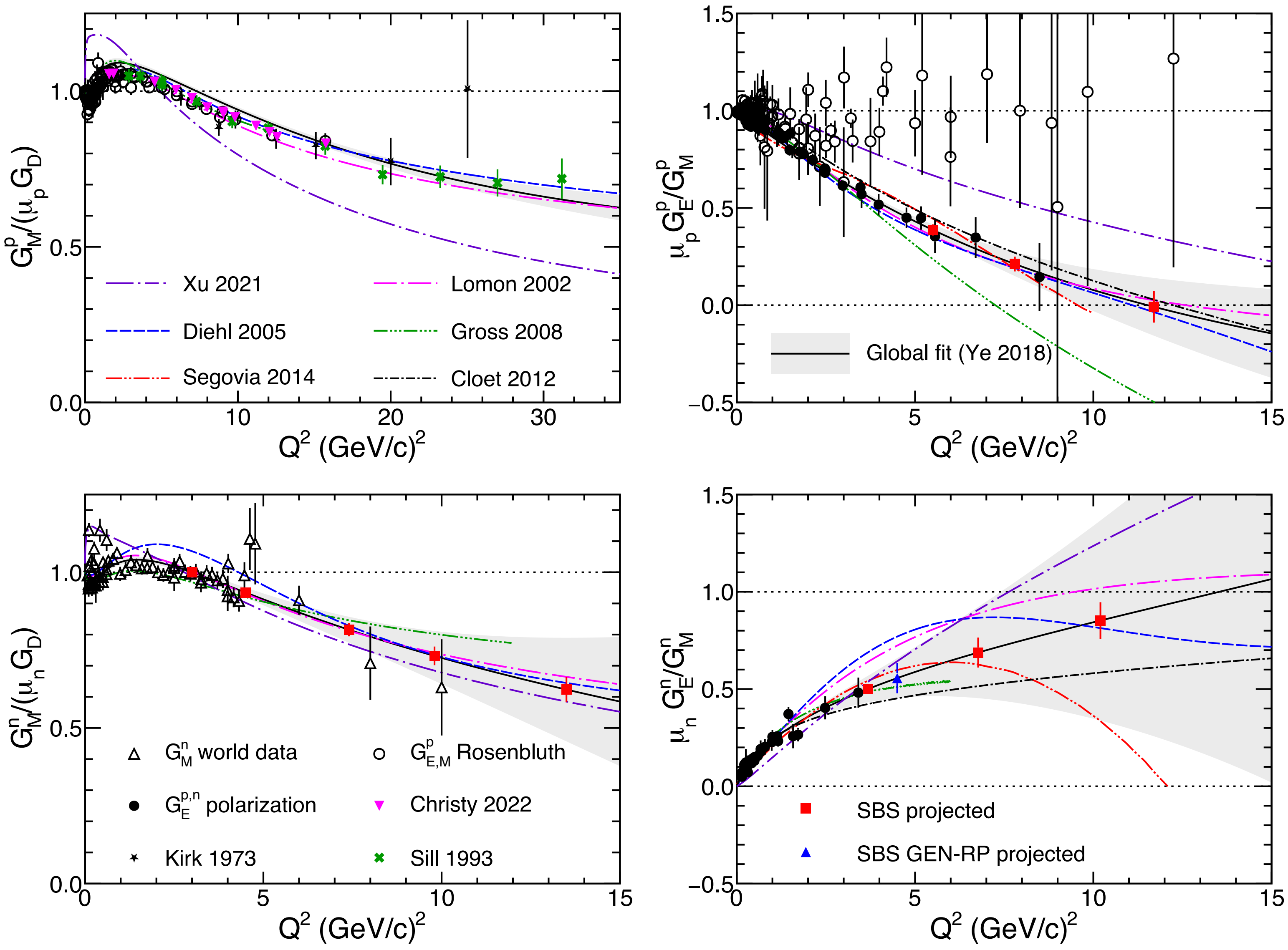

- Figure from "50 Years of QCD": : https://arxiv.org/abs/2212.11107
- GMN/nTPE (E12-09-019/E12-20-010): Completed Oct. 2021-Feb. 2022
- GEN Helium-3: ~60% complete as of this writing
- GEN-RP: Projected run summer 2023
- GEP: Projected run 2024

Prospects for high-Q^2 nucleon FFs with 22 GeV CEBAF

$$\frac{d\sigma}{dQ^2} = \frac{4\pi\alpha^2}{Q^4}\frac{E'}{E}\cos^2\left(\frac{\theta}{2}\right)\frac{\epsilon G_E^2 + \tau G_M^2}{\epsilon(1+\tau)}$$

$$\frac{d\sigma}{d\Omega_e} = \frac{{E'}^2}{\pi}\frac{d\sigma}{dQ^2}$$

Experiment Design Considerations

- Precision *ep* cross sections determine G_M^p→High luminosity, precision spectrometers, e.g., Hall C HMS/sHMS. Detect scattered electron. Invariant mass resolution sufficient for clean selection of elastic.
- Medium-acceptance spectrometers (SBS+BigBite/ECAL): σ_n/σ_p for G_M^n, polarization transfer for G_E^p, G_E^n, high-luminosity polarized ^{3}He for G_E^n.
- Large-acceptance spectrometers (CLAS12 or SOLID): polarized proton targets (e.g., NH_3)

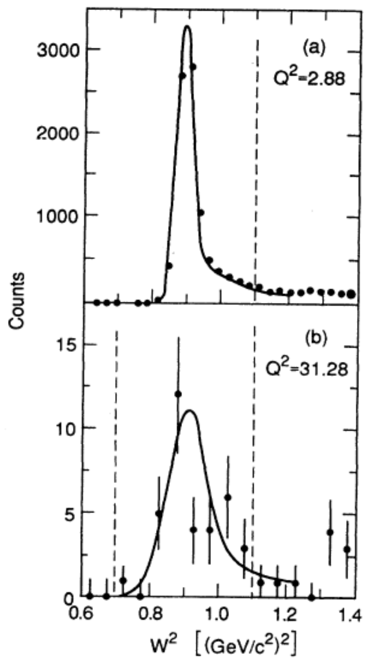

FIG. 19. Histograms of raw counts vs the missing mass squared at the highest and lowest values of Q^2 in this experiment. (a) $Q^2=2.883$ (GeV/c)^2. (b) $Q^2=31.28$ (GeV/c)^2. The curves show the expected resolution of the apparatus for each case, as determined from a Monte Carlo simulation of the experiment, including acceptance and radiative effects, but neglecting inelastic reactions. The data in each case show a clear peak with no significant background in the kinematically forbidden region of W^2 below the peak. The elastic radiative tail is visible above the peak. The data depart from the Monte Carlo curve near the threshold for pion production [$W^2=1.17$ (GeV/c)^2], as expected. The counts between the dashed vertical lines were summed to obtain the cross sections.

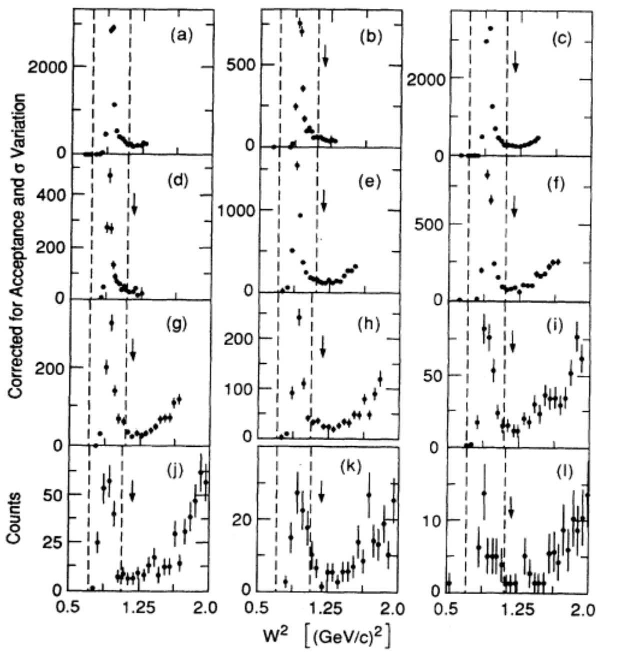

FIG. 20. Histograms of counts vs the missing mass squared corrected for the acceptance and summed over $\Delta\theta_{tot}$ as in Eq. (15). (a) $Q^2=2.9$ (GeV/c)^2, $\theta=21°$; (b) $Q^2=3.6$ (GeV/c)^2, $\theta=25°$; (c) $Q^2=5.0$ (GeV/c)^2, $\theta=21°$; (d) $Q^2=5.0$ (GeV/c)^2, $\theta=33°$; (e) $Q^2=7.3$ (GeV/c)^2, $\theta=21°$; (f) $Q^2=9.7$ (GeV/c)^2, $\theta=21°$; (g) $Q^2=11.9$ (GeV/c)^2, $\theta=21°$; (h) $Q^2=15.7$ (GeV/c)^2, $\theta=21°$; (i) $Q^2=19.4$ (GeV/c)^2, $\theta=21°$; (j) $Q^2=23.2$ (GeV/c)^2, $\theta=21°$; (k) $Q^2=27.0$ (GeV/c)^2, $\theta=25°$; (l) $Q^2=31.2$ (GeV/c)^2, $\theta=33°$. The threshold for pion production is marked by an arrow on these plots. Data points between the dashed lines were summed to yield the total counts N_{peak}. Counting rates in the kinematically forbidden region of W^2 below the lower cut value of 0.7 (GeV/c)^2 were negligible.

Sill, PRD, 48, 29 (1993): Note: highest SLAC beam energy was 21 GeV for these data

Elastic eN Scattering Kinematics for JLab 22

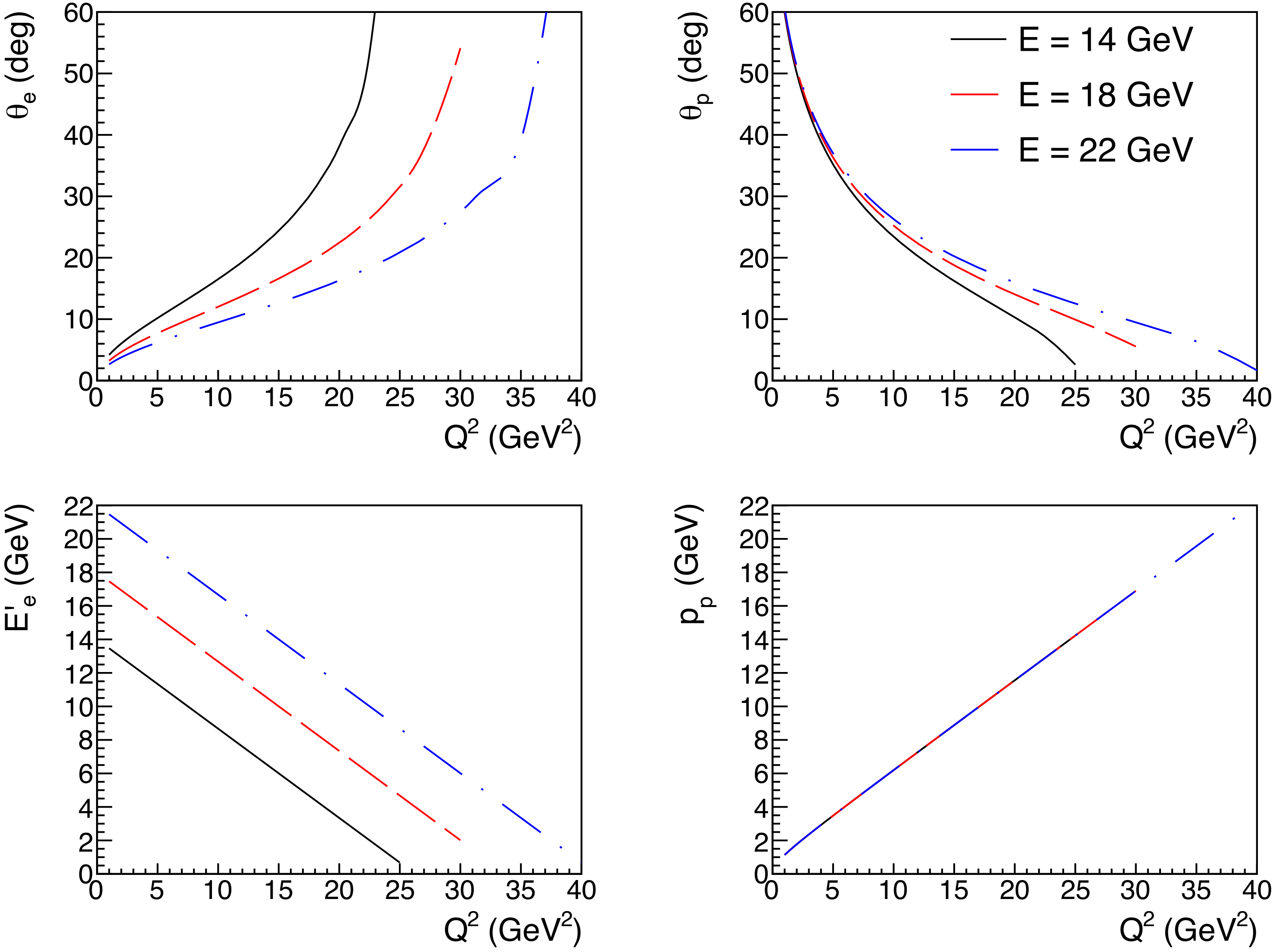

- Scattering angles are well matched to the acceptances of both small-acceptance and large-acceptance devices (CLAS12, SOLID, SBS+BigBite, HMS/SHMS)
- Particle momenta are rather high →
  - Challenge for Hall C spectrometers in some kinematic regions
  - Challenging in terms of resolution for large-acceptance spectrometers in some kinematic regions
- Nonetheless, even existing spectrometers should be able to cover a lot of new phase space

Virtual photon polarizations

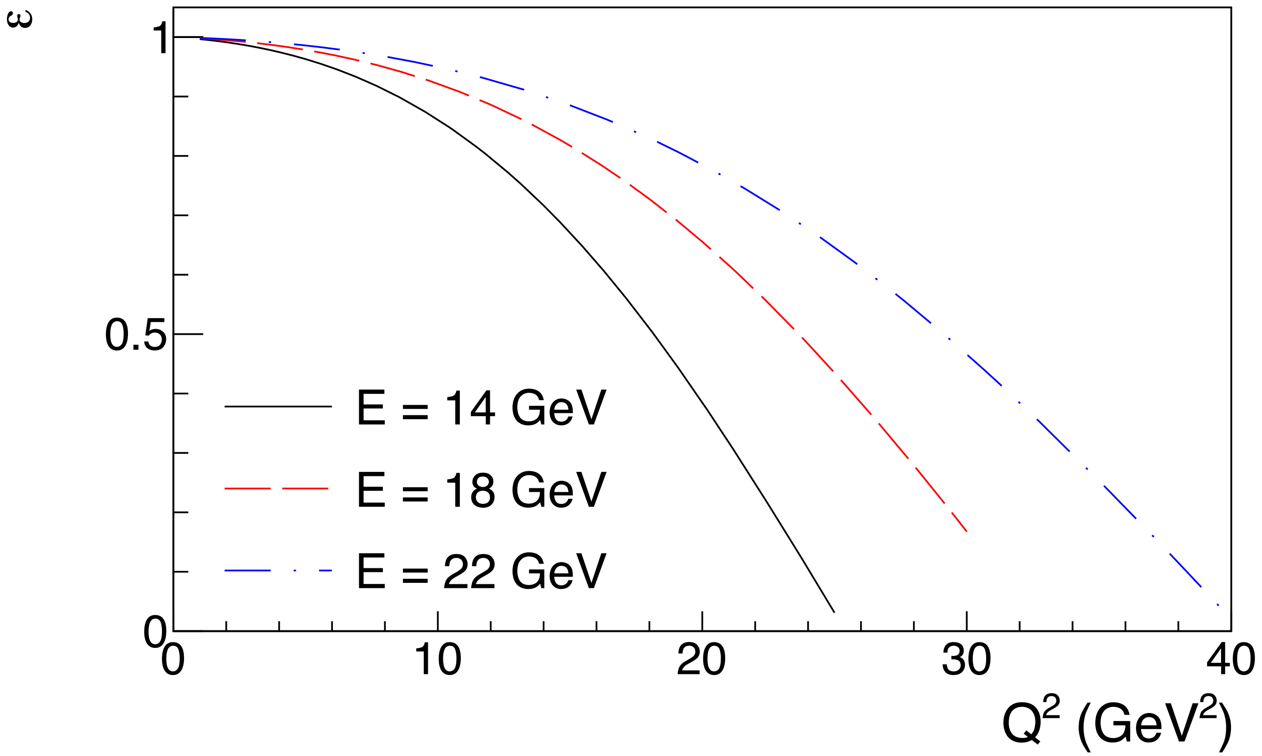

$$A_{eN} \equiv \frac{\sigma_+ - \sigma_-}{\sigma_+ + \sigma_-} = P_{\text{beam}} P_{\text{targ}} \left[A_t \sin\theta^* \cos\phi^* + A_\ell \cos\theta^*\right]$$

$$A_t = -\sqrt{\frac{2\epsilon(1-\epsilon)}{\tau}} \frac{r}{1 + \frac{\epsilon}{\tau} r^2}$$

$$A_\ell = -\frac{\sqrt{1-\epsilon^2}}{1 + \frac{\epsilon}{\tau} r^2}$$

$$r \equiv \frac{G_E}{G_M}$$

- Higher passes provide good lever arm in ϵ, for polarization observables and Rosenbluth separations in the range $10 \leq Q^2 \leq 30$ GeV²
- Optimal beam energy at a given Q^2 for polarization observables is $\epsilon \approx 0.5$
- **Unique to JLab; EIC always has $\epsilon \approx 1$**

Asymmetries/Polarizations: Proton

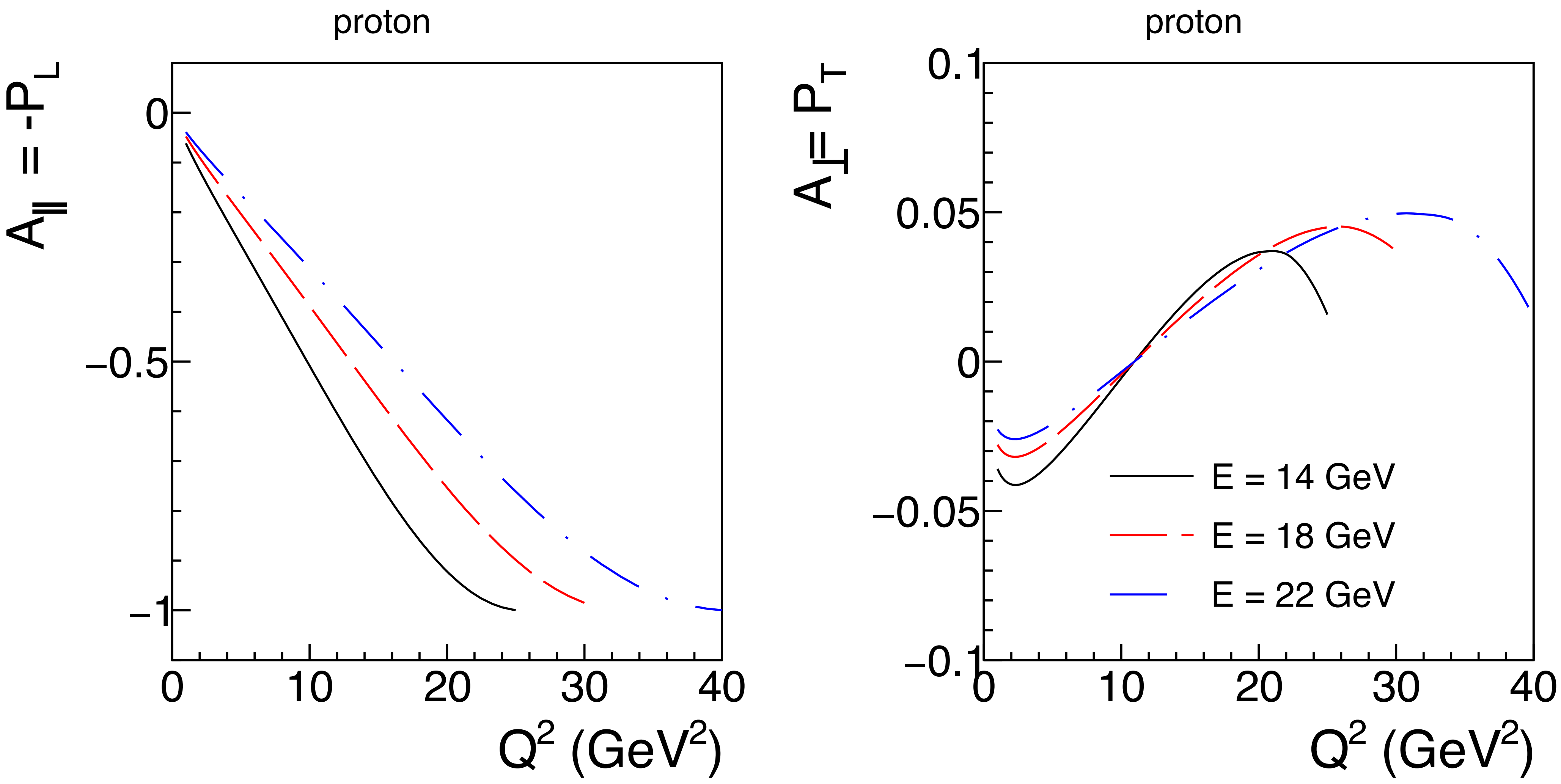

Different passes give optimal FOM for different Q^2's

Asymmetries/Polarizations: Neutron

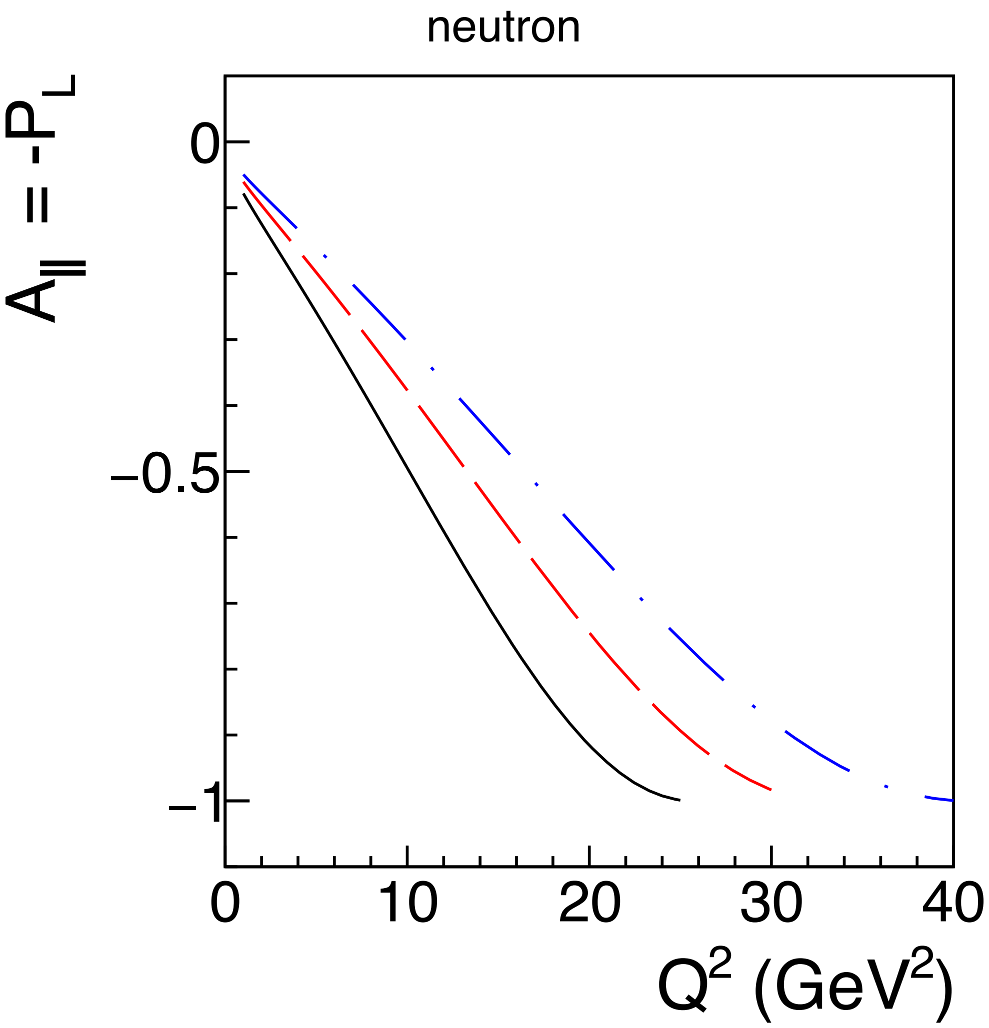

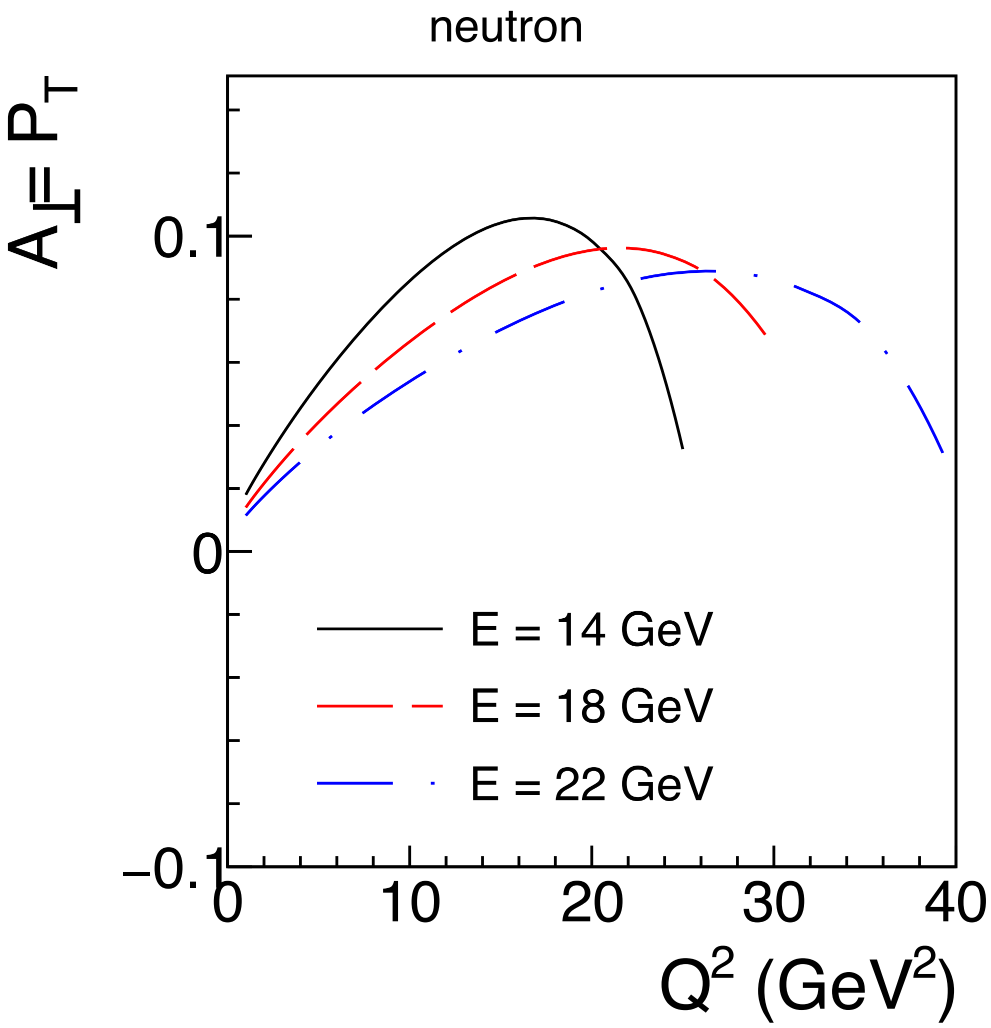

Different passes give optimal FOM for different Q^2's

Cross sections versus Q^2

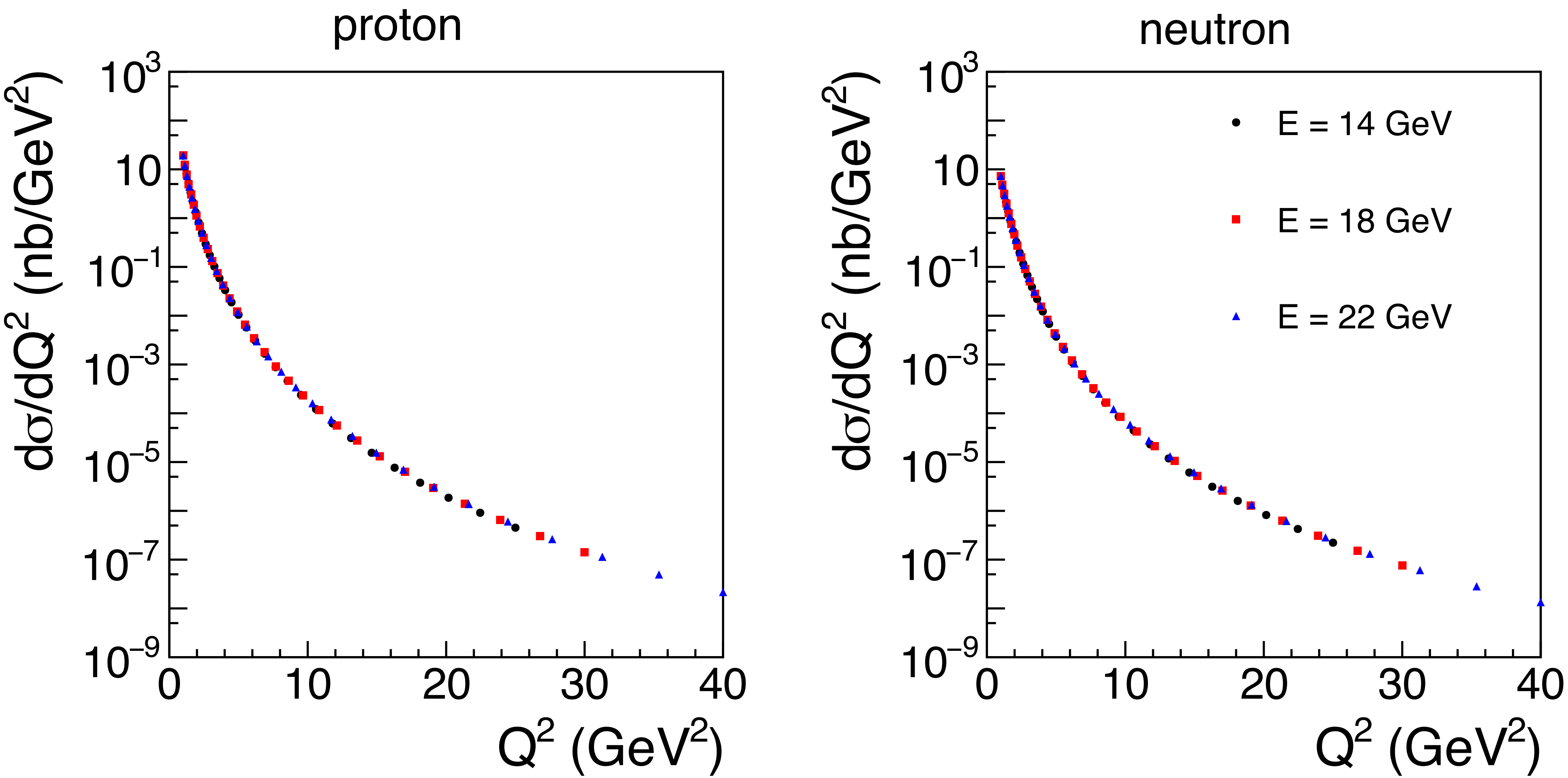

Note: Born cross section (no RC), assuming 2π azimuthal acceptance

Count rates versus Q^2

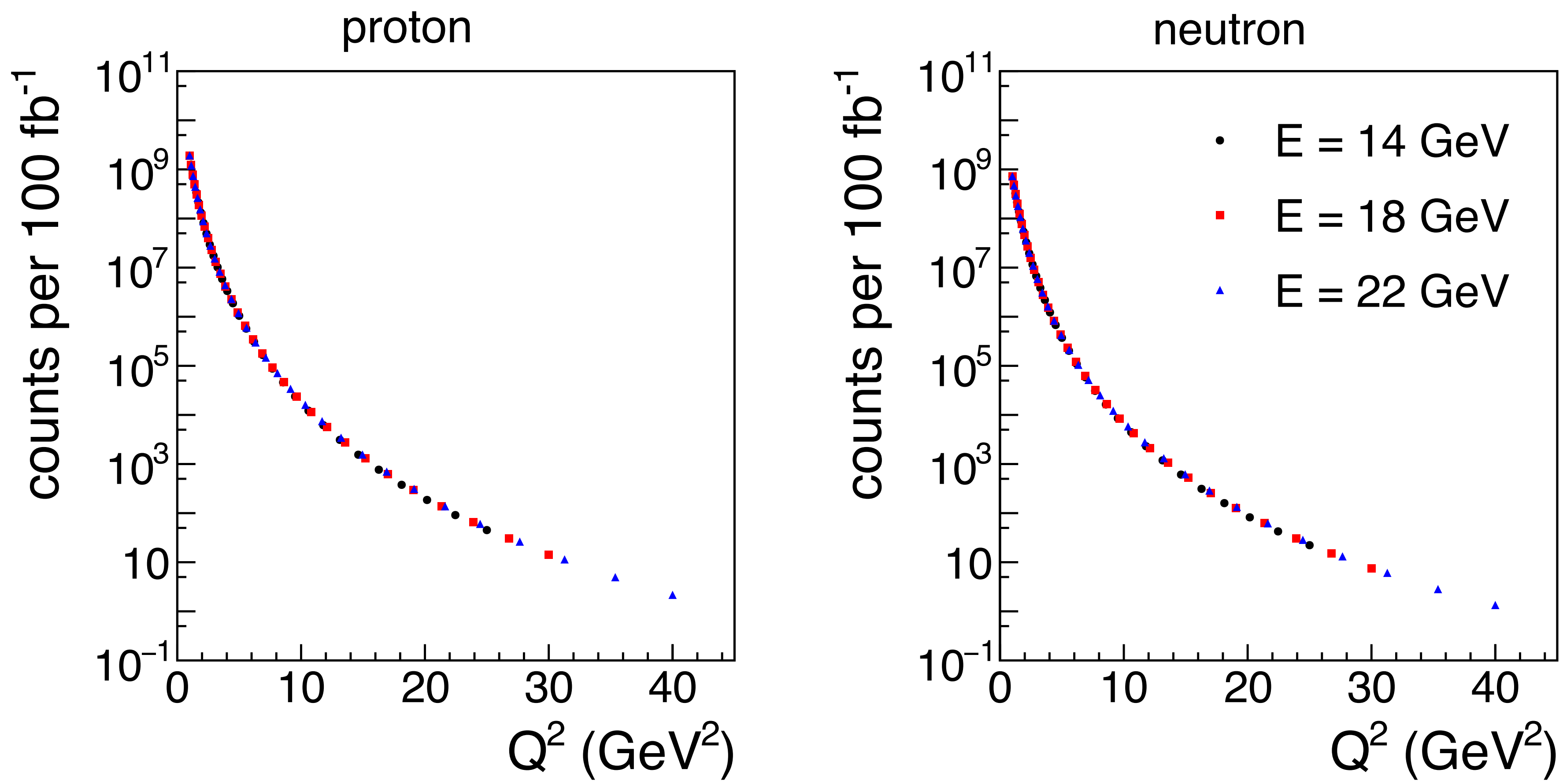

Luminosity (cm^{-2} s^{-1}, electron-nucleon)	fb^{-1}/day
10^{35} (NH_3/ND_3), polarized p/n	8.64
10^{37} (Helium-3 SEOP), polarized n	864
10^{38}-10^{39} (liquid hydrogen, deuterium)	8,640-86,400

Notes: assuming 2π azimuthal acceptance, Q^2 bin width $\approx Q^2$ spacing between points

- JLab high luminosity provides plenty of count rate up to max. accessible Q^2
- EIC ~100 fb^{-1} per YEAR (best-case)

Pion FF

Phase 1: Form Factor Projections

Garth Huber, huberg@uregina.ca

- Y-axis values of projected data are arbitrary
- The errors are projected, based on Δε from beam energies on earlier slides, and T/L ratio calculated with Vrancx Ryckebusch model
- Inner error bar is projected statistical and systematic error
- Outer error bar also includes a model uncertainty in the form factor extraction, added in quadrature
- F_π errors based on Fπ–2 and E12–19–006 experience
- F_K errors more uncertain, as E12–09–011 analysis not yet completed

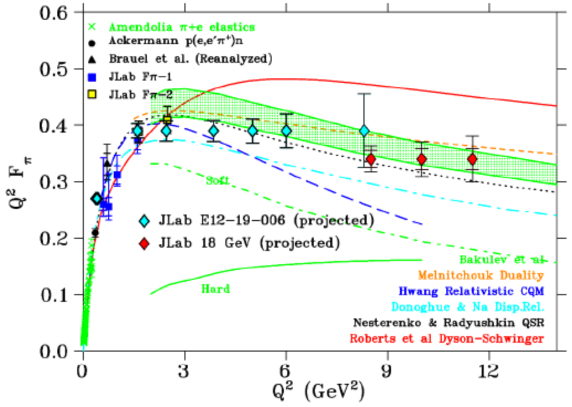

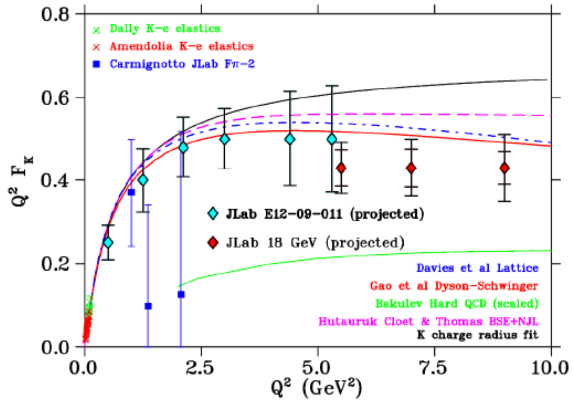

15

Importance of JLab F_π in EIC Era

Garth Huber, huberg@uregina.ca

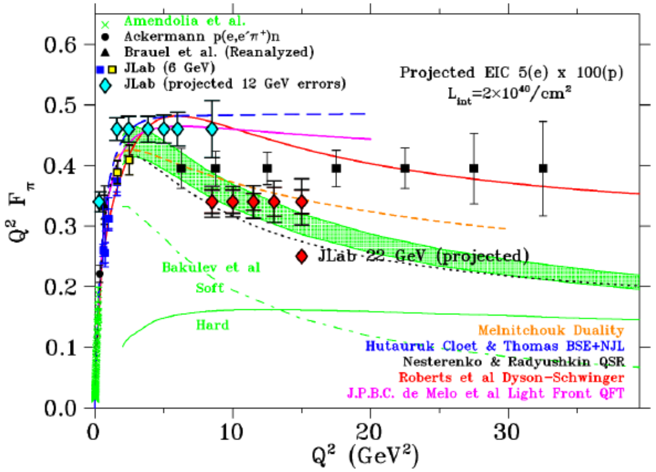

- Quality L/T-separations impossible at EIC (can't access ε<0.95)
- JLab will remain ONLY source of quality L–T separated data!
- **Phase 2: 22 GeV beam with upgraded HMS'**
  - Extends region of high quality F_π values to Q²=13 GeV²
  - Somewhat larger errors to Q²=15 GeV²
- Provides MUCH improved overlap of F_π data set between JLab and EIC!

20

Summary and Conclusions

- High-Q^2 hadron elastic FFs (nucleon/pion/kaon) continue to attract major theoretical and experimental interest—simple, clean theoretical definition and interpretation; precision benchmark for QCD theory and all phenomenological models
- SBS program (~50% complete as of today), will dramatically improve and reshape our understanding of the nucleon.
- Prediction: SBS GEP measurement at 12 GeV^2, despite impressive precision and Q^2 reach will not conclusively establish a statistically significant zero crossing → JLab 22 will easily get us to 20-25 GeV^2 for G_E^p, G_E^n and to 30+ GeV^2 for G_M^p, G_M^n with excellent precision→ EIC will never be able to do this (see, however, https://arxiv.org/abs/2207.04378)
- JLab 22 can do precise L/T separated $p(e,e'\pi^+)n$ to 15 GeV^2 → Unique capability
- ***If*** hadron elastic FFs at very large Q^2 continue to be theoretically interesting and important, JLab 22 GeV upgrade is the ONLY way to do these measurements!

Backups

Unexpected behavior of Pauli/Dirac flavor FF ratios

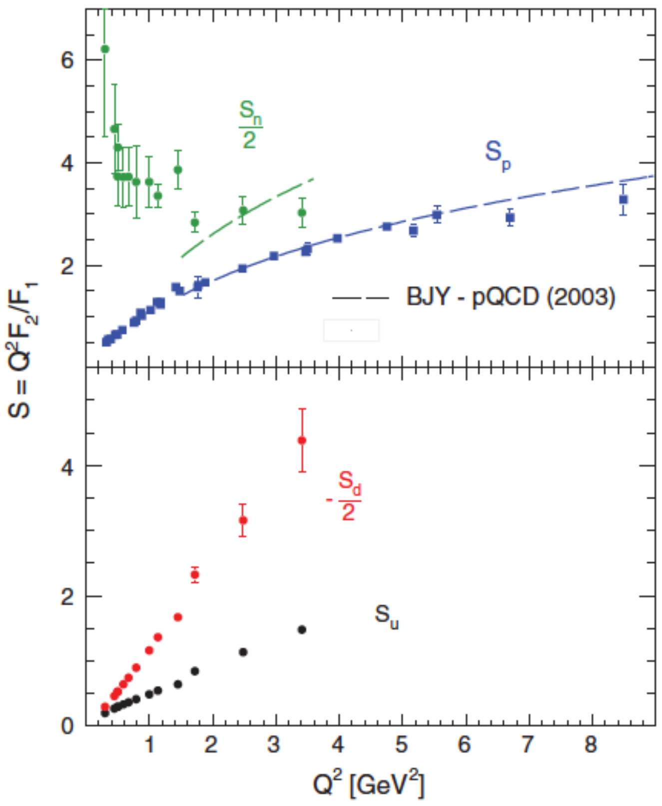

FIG. 1 (color). The ratio of the Pauli and Dirac form factors, multiplied by Q^2, $S = Q^2F_2/F_1$, vs the negative four-momentum transfer squared Q^2. The upper panel shows S_p for the proton and S_n for the neutron using data from Refs. [16–21], as well as the curves of the prediction [12]: $\ln^2[Q^2/\Lambda^2]$ for $\Lambda = 300$ MeV, which is normalized to the data at 2.5 GeV^2. The bottom panel shows the individual flavor quantities S_u and S_d for the u and d quarks, respectively.

Fit function (proton): $\frac{F_2}{\kappa_p F_1} = \frac{N(1+p_1\tau)}{1+q_1\tau+q_2\tau^2}$

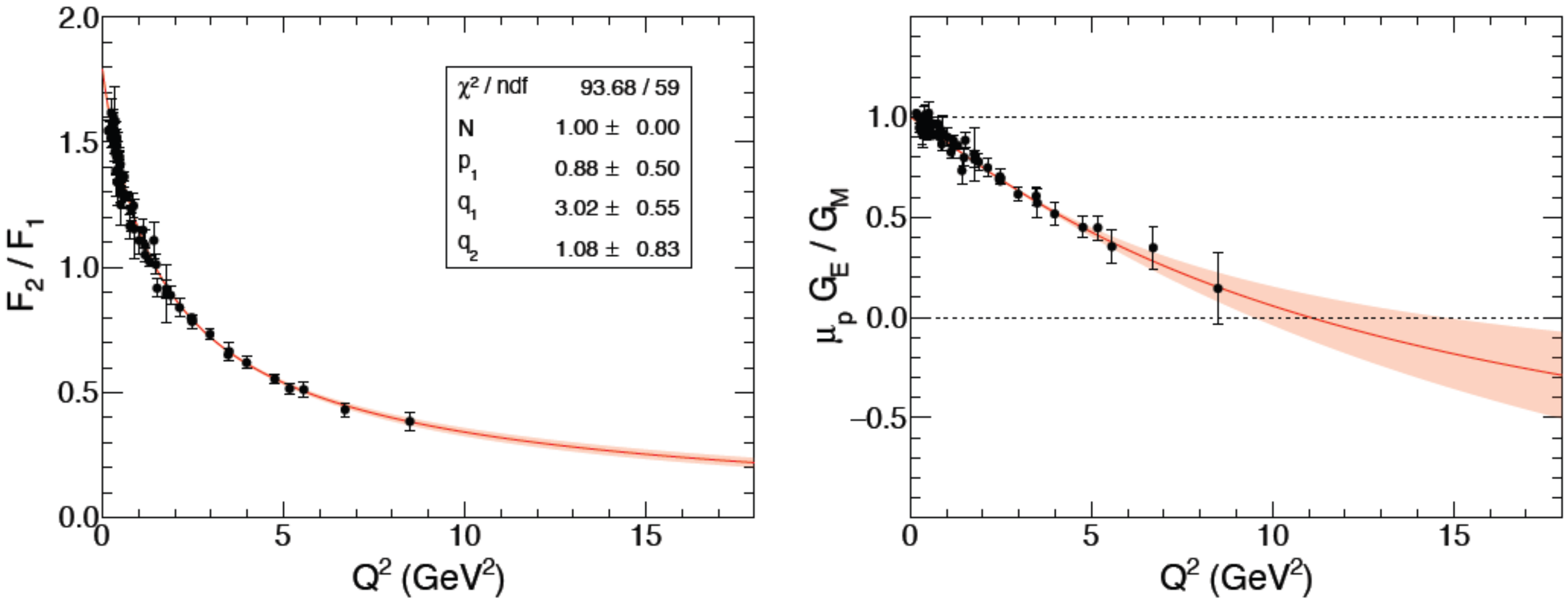

- Naïve pQCD prediction for asymptotic large-Q^2 behavior of Pauli/Dirac FF ratio is $\frac{F_2}{F_1} \propto \frac{1}{Q^2}$ based on helicity conservation in high-energy scattering on ~massless quarks.
- Flavor FF ratios almost constant above 1 GeV² –consistent with theories in which "soft" diquark correlations play an important role in the structure

Polarization Transfer Concept

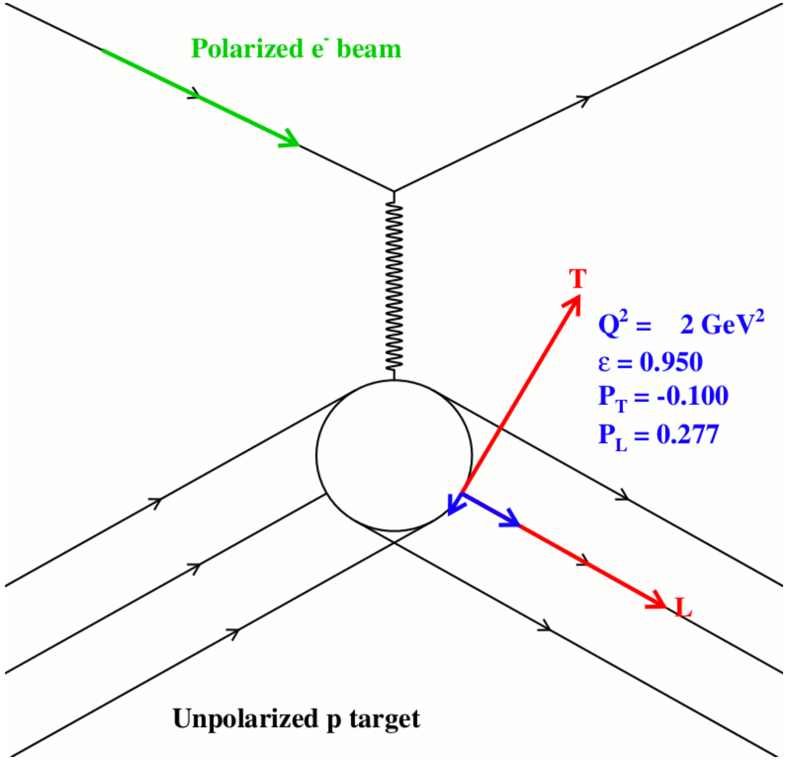

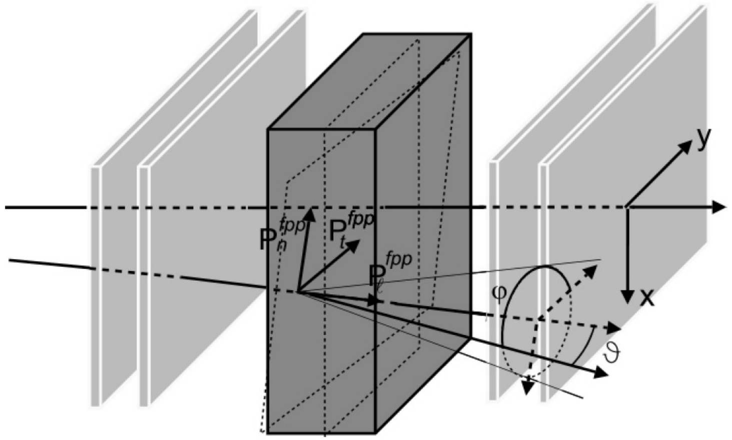

FIG. 9. Principle of the polarimeter, showing a noncentral trajectory through the front chambers, scattering in the analyzer, and a track through the back chambers; ϑ is the polar angle, and φ is the azimuthal angle from the y direction counterclockwise.

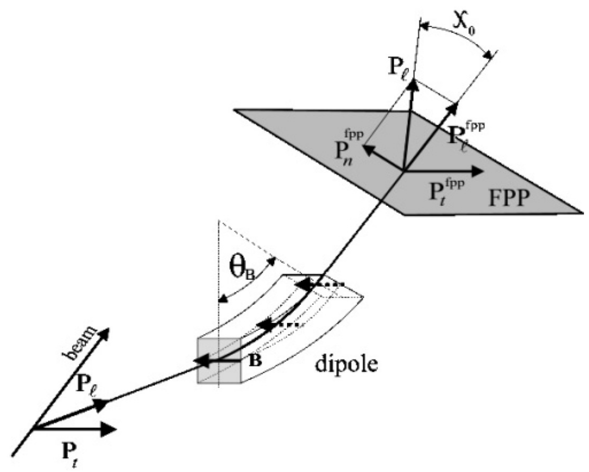

FIG. 15. Precession of the polarization component P_ℓ in the dipole of the HRS by an angle χ_θ.

- Based on spin-orbit coupling in proton-nucleus scattering

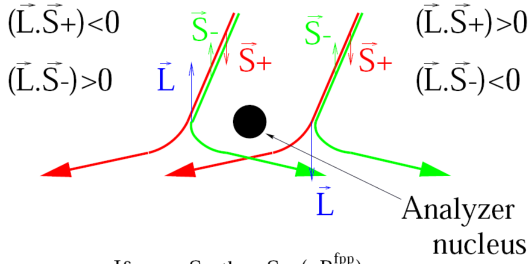

If more S+ than S- $(+P_x^{fpp})$ ...

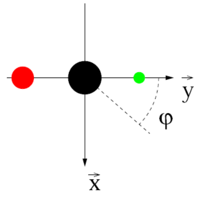

... more events left than right

- A spin-1/2 particle, such as a proton, is preferentially deflected by the nuclear spin-obrit force along the direction of $\vec{p}\times\vec{S}$, where $\vec{p}$ is the incident proton momentum, and $\vec{S}$ is the proton spin.
  - A spin-orbit force is insensitive to longitudinal polarization!
  - Precession in a magnetic field rotates P_L into a transverse component that can be measured
- Azimuthal asymmetry in the angular distribution of secondary scatterings measures $\vec{S}$